NASA TECHNICAL NOTE

NASA TN D-3903

NASA TN D-3903

FLIGHT-TEST EVALUATION OF AN ON-OFF RATE COMMAND ATTITUDE CONTROL SYSTEM OF A MANNED LUNAR-LANDING RESEARCH VEHICLE

by Calvin R. Jarvis

Flight Research Center
Edwards, Calif.

NATIONAL AERONAUTICS AND SPACE ADMINISTRATION • WASHINGTON, D. C. • APRIL 1967

NASA TN D-3903

FLIGHT-TEST EVALUATION OF AN ON-OFF RATE COMMAND ATTITUDE CONTROL SYSTEM OF A MANNED LUNAR-LANDING RESEARCH VEHICLE

By Calvin R. Jarvis

Flight Research Center
Edwards, Calif.

NATIONAL AERONAUTICS AND SPACE ADMINISTRATION

For sale by the Clearinghouse for Federal Scientific and Technical Information
Springfield, Virginia 22151 – CFSTI price $3.00

FLIGHT-TEST EVALUATION OF AN ON-OFF RATE COMMAND ATTITUDE CONTROL SYSTEM OF A MANNED LUNAR-LANDING RESEARCH VEHICLE

By Calvin R. Jarvis
Flight Research Center

SUMMARY

The control characteristics of a free-flight lunar-landing research vehicle (LLRV) which uses a "fly-by-wire" on-off rate command attitude control system have been investigated. Results of a flight-test program and fixed-base simulator studies show that the rate command control boundary associated with vehicle attitude control in a lunar-gravity environment can be expanded from that experienced in conventional VTOL operation to include less damping, lower control authorities, and higher controller sensitivities. Satisfactory LLRV attitude control was attained at pitch and roll control authorities as low as 5 deg/sec^2 (0.09 rad/sec^2) and 7.5 deg/sec^2 (0.13 rad/sec^2), respectively. Flight experience showed that disturbing moments and low values of control authority could result in pilot-induced instabilities about the pitch and roll axes as a result of the control-logic arrangement of the LLRV. For this reason, the degree to which the maximum disturbing moments could be controlled was the limiting factor in establishing the minimum level of control authority for satisfactory operation.

The large vehicle attitudes and long lead times required for translation maneuvers in the lunar-simulation mode were initially distracting to pilots. Pilots accepted higher controller sensitivities for lunar-simulation operation than for conventional VTOL operation.

INTRODUCTION

The present goal of the Apollo space program has greatly expanded this country's research effort in many areas. One of these areas is the definition of the basic attitude control requirements for accomplishing a manned landing on the moon. Until recently, experience with VTOL vehicles was based entirely on the earth's gravitational and atmospheric environments. In 1962, a six-degree-of-freedom fixed-base simulator program was conducted (ref. 1) to assess the handling qualities of a lunar-landing vehicle. These results were found to disagree markedly with similar studies for vehicles operating in an earth gravitational environment (refs. 2 to 4).

A clear-cut method of extrapolating the handling qualities and control requirements for a lunar vehicle from earth-referenced results does not exist. Since preliminary results from fixed-base simulator programs indicated a difference between

the control requirements for earth and lunar landing tasks, further studies were necessary to investigate pilot controllability of a vehicle in the lunar environment and to establish flying-quality requirements for safe, efficient lunar landings. For this purpose, the NASA Flight Research Center procured and developed, under contract, a free-flight lunar-landing research vehicle. The vehicle, which makes use of a vertically mounted jet engine to create a pseudolunar gravity field, was designed specifically to investigate the man-system requirements dictated by the final phase of a lunar mission. However, because of minimum aerodynamic effects, the LLRV is also a unique vehicle for use in earth-referenced VTOL control-system investigations. Thus, the vehicle offers an ideal means of comparing flight experience and handling qualities for specific control parameters in both earth- and lunar-gravity environments.

This paper deals specifically with the evaluation of the capability of an on-off rate command attitude control system to provide satisfactory control for maneuvering a vehicle in a lunar-gravity environment. Control boundaries, based on pilot ratings, are established from fixed-base simulator studies that define satisfactory values of rate dead band, controller sensitivity, and angular acceleration. These boundaries are then compared to flight results obtained with the LLRV. Results are presented for both earth- and lunar-oriented operation.

SYMBOLS

Measurements for this investigation are given, where applicable, in both the U. S. Customary Units and the International System of Units (SI). Details concerning the use of SI, together with physical constants and conversion factors, are given in reference 5.

A, B, C, D	pitch and roll attitude-rocket designations
E, F, G, H	yaw attitude-rocket designations
d	rate dead band, deg/sec (rad/sec)
e^{-st}	transport delay
G	rate-gyro gain
g	acceleration due to earth's gravity, 32.2 ft/sec^2 (9.80 m/sec^2)
I	inertia, slug-ft^2 (kg-m^2)
K	controller sensitivity, $\frac{\text{Rate commanded}}{\text{Controller deflection}}$, sec^{-1}
L	control moment, ft-lb (N-m)
N	nonlinear describing function
$R = \frac{d}{2X}$	

s	Laplace operator
t	time, sec
W	vehicle weight, lb (N)
$\dot{w}$	rate of attitude-rocket propellant consumption, lb/sec (kg/sec)
X	input amplitude to nonlinear element
x	longitudinal displacement, ft (m)
$\ddot{x}$	forward acceleration, ft/sec^2 (m/sec^2)
Y	output amplitude of nonlinear element
y	lateral displacement, ft (m)
δ	controller deflection, deg (rad)
Θ	pitch attitude, deg (rad)
$\dot{\Theta}$	pitching angular rate, deg/sec (rad/sec)
$\ddot{\Theta}$	pitching angular acceleration, deg/sec^2 (rad/sec^2)
τ_1	rocket time constant, sec
τ_2	filter time constant, sec
$\dot{\varphi}$	rolling angular rate, deg/sec (rad/sec)
$\ddot{\varphi}$	rolling angular acceleration, deg/sec^2 (rad/sec^2)
ω	frequency, rad/sec

Subscripts:

pedal	yaw pedal
S	standard attitude rockets
stick	control stick
T	test attitude rockets
1,2	limit-cycle amplitudes
Θ	pitch axis
φ	roll axis

DESCRIPTION OF THE LUNAR-LANDING RESEARCH VEHICLE

Vehicle

The LLRV is a 3600-pound (1633-kilogram) vehicle designed specifically to investigate problems associated with the terminal phase of a manned lunar landing. The principal propulsion system of the LLRV is a General Electric CF700-2V turbojet engine. The vehicle structure consists of a tubular framework and sheet-metal truss construction. The pilot's controls and flight instruments are in the forward-mounted pilot's compartment, which is situated approximately 6 feet (2 meters) above the ground. The aft equipment platform contains electronic control equipment, a radar altimeter, a Doppler radar for measuring velocity, and electronics instrumentation. A photograph of the LLRV is presented in figure 1.

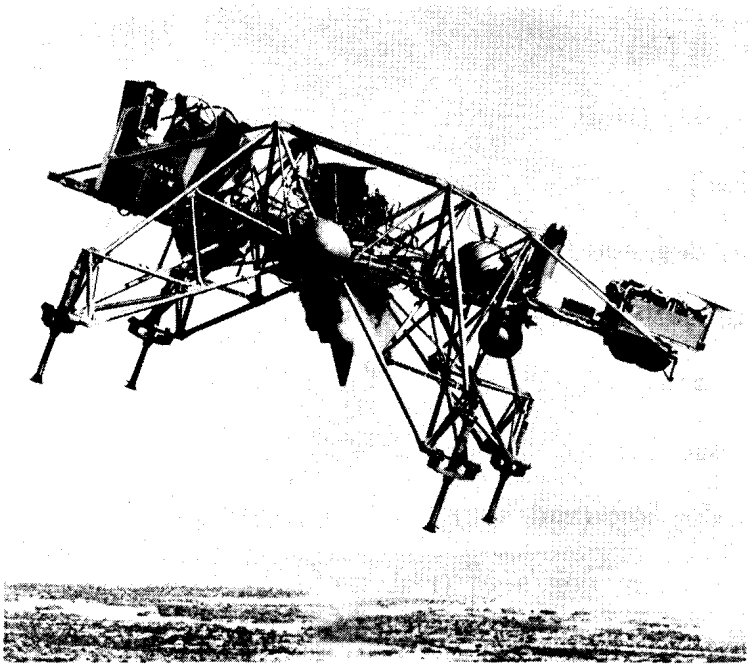

Figure 1.– Lunar-landing research vehicle. E-14570

The vehicle framework is connected to the jet engine through a large movable-gimbal arrangement. The gimbals allow the engine to remain essentially vertical, independent of the vehicle attitude. The thrust and attitude of the engine are controlled automatically in the lunar-simulation mode of operation. The aerodynamic drag forces are automatically opposed so that the vehicle responds as though in a vacuum, and five-sixths of the vehicle weight is supported by the jet to simulate lunar gravity. The pilot controls the thrust of two hydrogen-peroxide lift rockets to support the remaining one-sixth of the vehicle weight and to regulate the rate of descent. Horizontal translation is initiated and terminated by pitching or rolling the vehicle to tilt the rocket lift vector. While the vehicle is pitched or rolled in the lunar mode, the engine remains vertical except for the small deviations required to oppose drag forces.

A comparison of LLRV operation during a lunar-simulation maneuver with conventional helicopter operation is shown in figure 2. Assuming that the weight of the two vehicles is equal, a forward acceleration $\dot{x}$ is generated by tilting the helicopter's rotor thrust vector through an angle of 5° (0.09 rad). To generate an equivalent $\dot{x}$ acceleration, the LLRV must tilt at an angle of approximately 30° (0.52 rad), since only the lift-rocket thrust is being vectored. The engine remains vertical, while supporting five-sixths of the weight of the LLRV, except for small angles required for drag compensation.

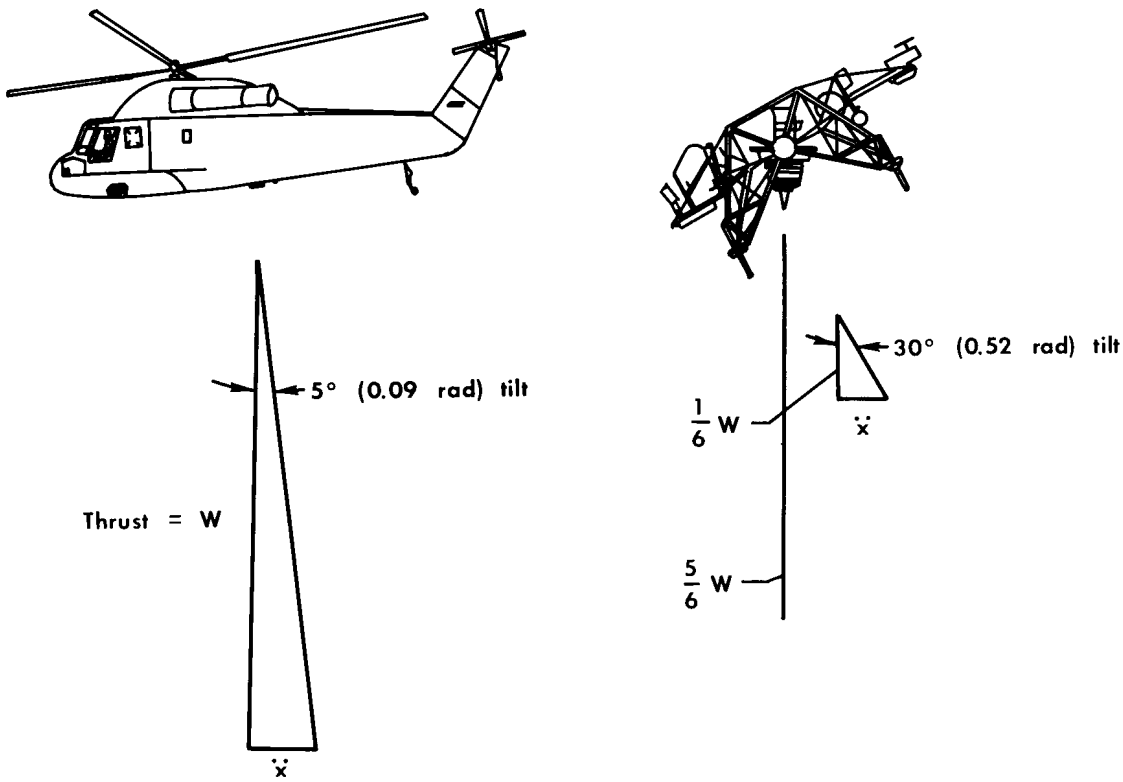

Figure 2.– Comparison of conventional helicopter and LLRV operation.

The LLRV can also be operated in a conventional VTOL mode with the engine hydraulically locked along the vertical body axis of the vehicle. The engine then tilts with changes in vehicle attitude, and translation is accomplished by vectoring the large jet thrust.

A detailed discussion of the vehicle hardware is presented in reference 6.

Attitude Control System

The LLRV attitude control system evaluated in this study is an on-off, rate command, fly-by-wire system which uses 16 hydrogen-peroxide attitude rockets to provide the necessary control moments. The attitude rockets are located in clusters of four about the vehicle. Firing signals for the rockets are generated by the electronic system in response to inputs from conventional center stick and rudder pedals and from rate gyros. The 16 attitude rockets are separated into two independent sets of eight, designated as standard and test. Each set has completely separate plumbing and power supplies. The pilot can select either or both sets. The thrust level for each rocket is fixed for a given flight but can be ground adjusted from 18 pounds to 90 pounds (80 newtons to 400 newtons).

Force-gradient characteristics of the LLRV center stick and yaw pedals are shown in figures 3(a) and 3(b), respectively. The range of controller sensitivities evaluated during this study is shown in figures 4(a) and 4(b). As can be seen in figure 4, a

1° stick mechanical dead band was used in pitch and roll and a 2° pedal mechanical dead band was used in yaw.

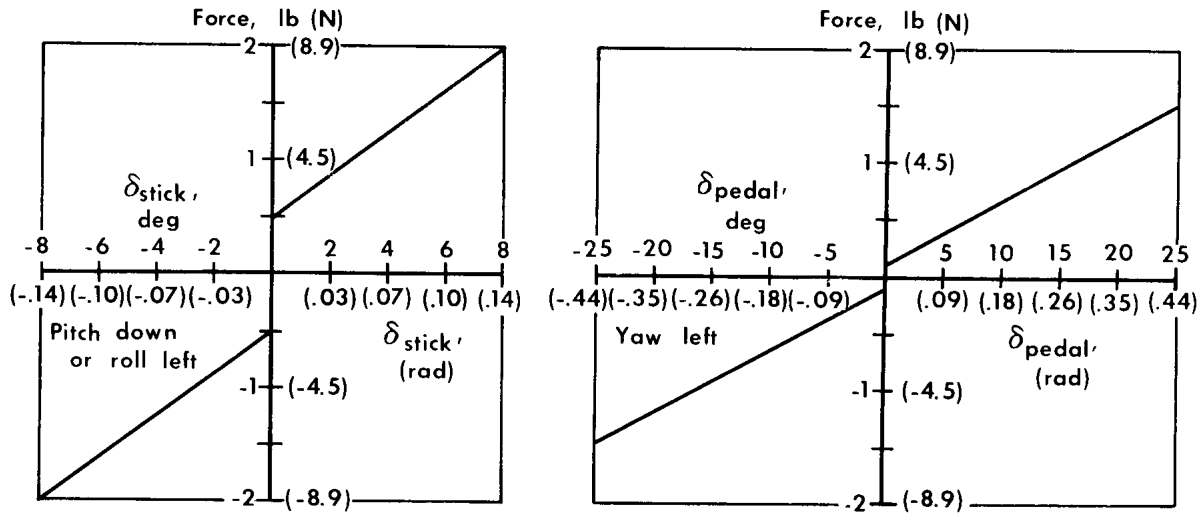

(a) Center stick (pitch and roll).

(b) Yaw pedals.

Figure 3.– LLRV center-stick and yaw-pedal force gradients.

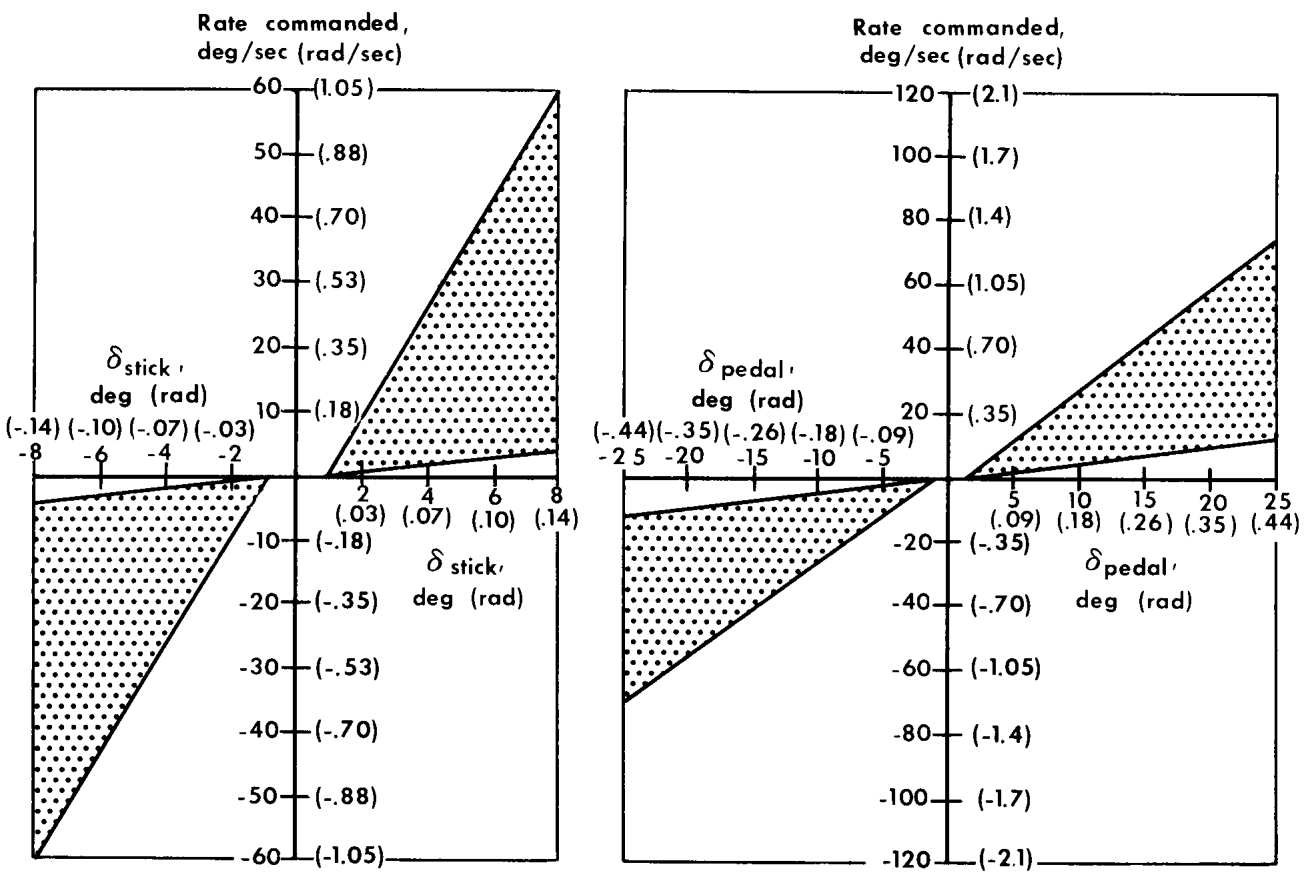

(a) Pitch and roll.

(b) Yaw.

Figure 4.– Range of LLRV controller sensitivities used during evaluation of rate command system.

A block diagram showing the basic elements of the rate command system in each of the orthogonal body-axis planes is presented in figure 5. Rate gyros provide feedback in a conventional manner which is summed, negatively, with the pilot command signal. The resultant error signal is then applied to the input of a switching amplifier which is triggered when the resultant error signal exceeds a threshold level proportional to vehicle angular rate. The switching-amplifier output is then used to operate on-off solenoid valves that control the flow of propellant to the attitude rockets.

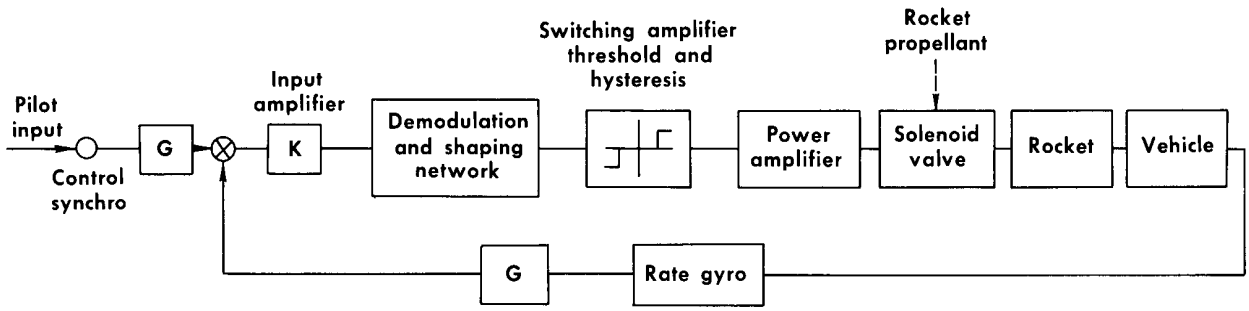

Figure 5.– Simplified block diagram of LLRV rate command attitude control system (similar diagram for all three axes).

Attitude-rocket layout, nomenclature, and possible combinations in the redundant modes with which to achieve a desired motion are shown in figure 6. All the pitch

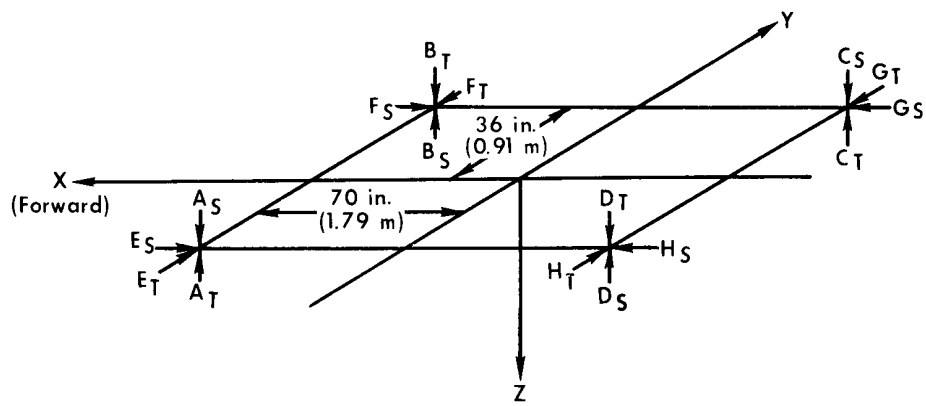

Rockets with subscript S denote standard rockets fire.
Rockets with subscript T denote test rockets fire.
For dual-system operation, both standard and test rockets fire.

Rocket		A_S	A_T	B_S	B_T	C_S	C_T	D_S	D_T	E_S	E_T	F_S	F_T	G_S	G_T	H_S	H_T
Pitch	Up		✓	✓		✓			✓								
	Down	✓			✓		✓	✓									
Roll	Right		✓		✓	✓		✓									
	Left	✓		✓			✓		✓								
Yaw	Right										✓	✓			✓	✓	
	Left									✓			✓	✓			✓
Pitch up and roll right			✓			✓											
Pitch up and roll left				✓					✓								
Pitch down and roll right					✓			✓									
Pitch down and roll left		✓					✓										

Figure 6.– Firing logic of the attitude control rockets.

rockets and the test yaw rockets are positioned 70 inches (1.79 meters) from the axis of rotation. All the roll rockets and the standard yaw rockets are 36 inches (0.91 meter) from the axis of rotation. The standard rockets are ground adjusted to produce a satisfactory control authority for the pilot. The test rockets are adjusted through the thrust range to investigate a representative interval of control authorities. To produce maximum control authorities, the two systems are actuated simultaneously. For combined pitch-roll inputs, the logic for each rocket system is arranged so that only one rocket fires, causing both a pitch and a roll moment to be applied to the vehicle. Since only one rocket fires for combined inputs when one rocket system is being used, the resultant control authority is one-half that obtained for single inputs.

In addition to the adjustable attitude-rocket thrust, other variable parameters include controller sensitivity, rate-gyro feedback gain, system hysteresis, and rate dead band. A more detailed discussion of the circuitry and operating characteristics of the LLRV attitude control system is presented in reference 7.

Pilot Displays

A photograph of the LLRV cockpit and instrument panel is presented in figure 7. A detailed description of the various instruments is given in reference 6. Vertical-scale instruments present normal acceleration, vertical velocity, and altitude. A three-axis ball displays attitudes and vernier indications of forward and side velocity on cross-pointers. A separate longitudinal- and lateral-velocity indicator with cross-pointers is also used. Additional displays were a pressure altimeter, a vertical-speed indicator, a clock, and annunciator lights.

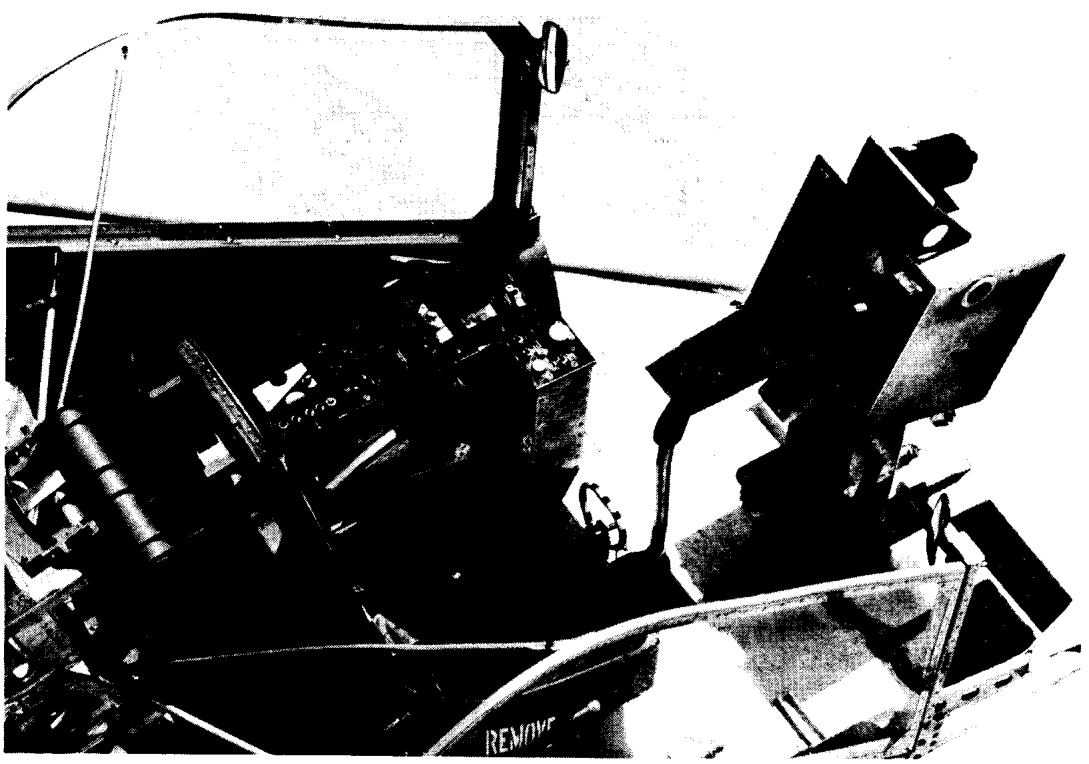

Figure 7.– LLRV cockpit and instrument panel. E-13115

Control Tasks

Lunar-landing-simulation maneuver. – An altitude profile of the landing maneuver used to evaluate LLRV handling qualities at various control-parameter settings is shown in figure 8. The task calls for lift-off in the gimbal-locked (VTOL) mode and a longitudinal translation and climbout to an altitude of approximately 200 feet (61 meters) over a ground marker. At this point, a 90° (1.57 rad) heading change is executed, and a hover is established. Transition is then made into the lunar-simulation mode, and the pilot maintains a hover by using lift-rocket thrust. The vehicle is then pitched down and a longitudinal translation and descent maneuver established toward a ground marker 800 feet (244 meters) in front of the vehicle. The forward velocity is reduced by pitching the vehicle up, and a hover is established approximately 10 feet (3.1 meters) over the landing marker. The pilot then manipulates the vehicle so that a landing is accomplished as close to the marker as possible. Translation velocities and sink rates generally were held to less than 10 ft/sec (3.1 m/sec) and vehicle attitude angles were kept less than 10° (0.18 rad) throughout the landing maneuver. The pilot rated the handling characteristics of the vehicle by using the rating scale shown in table I. The pilot was also requested to distinguish between a hover rating and a translation rating when such a distinction existed.

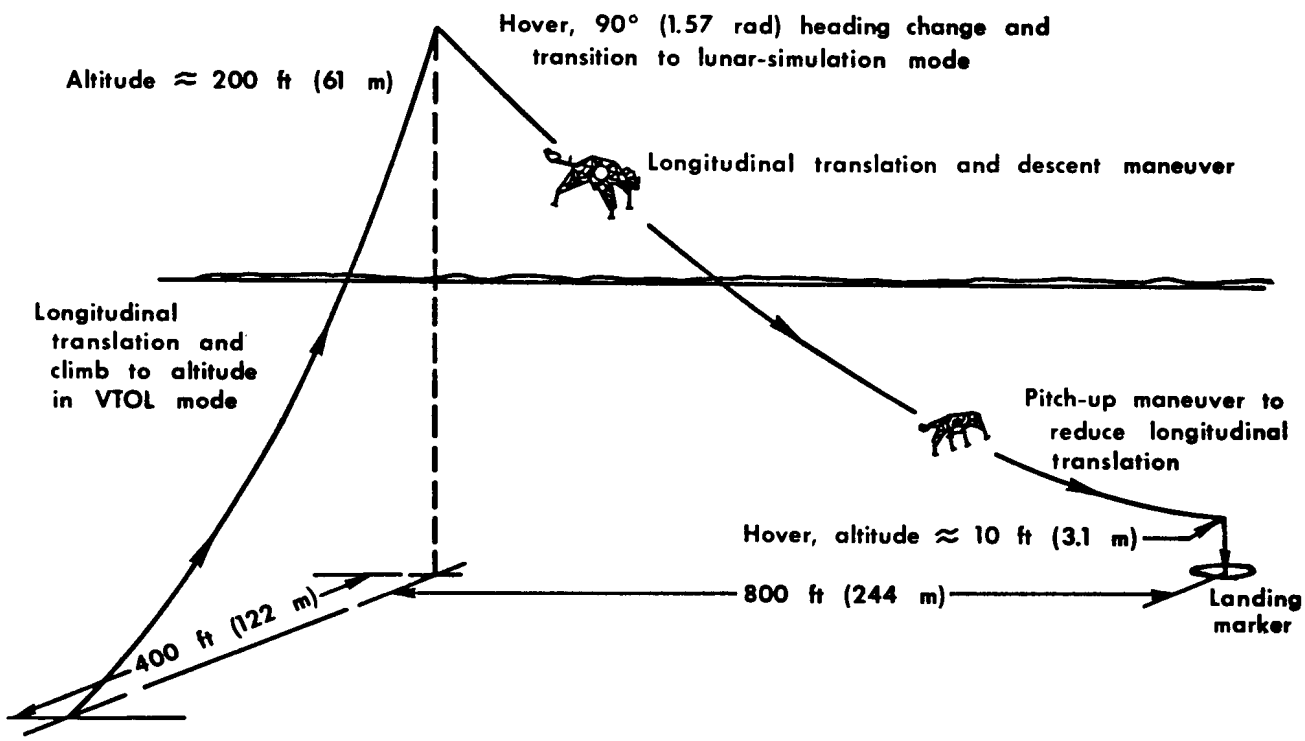

Figure 8.– Lunar-landing-simulation maneuver.

Large-angle maneuver. – Early in the evaluation of the rate command system, it became apparent that a particular set of control parameters would have satisfactory control characteristics for the previously defined lunar-landing-simulation maneuver but would be unsatisfactory for larger vehicle attitudes and translational velocities. In order to assess this problem more thoroughly, a second task, referred to as a large-angle maneuver, was investigated. The additional task essentially allowed the pilot a

free hand in evaluating the handling characteristics of the vehicle at attitudes greater than 10° (0.18 rad) and translational velocities greater than 10 ft/sec (3.1 m/sec).

Gimbal-locked mode. – Similar tasks performed in the lunar-simulation mode were also accomplished in the gimbal-locked or conventional VTOL mode of operation. Comparisons were then made between the control boundaries established for both 1 g and simulated 1/6 g operation. This task also resulted in a good assessment of the pilot's use of motion cues in controlling the vehicle and the relative changes in these cues from one mode to another.

LLRV fixed-base simulator. – A six-degree-of-freedom fixed-base analog simulator was used initially to establish the control boundaries for satisfactory operation of an on-off rate command system in lunar and earth gravitational environments. LLRV flight-test results were used to verify the control boundaries established from the simulator results. These simulator tests reduced the number of actual flights necessary to establish and verify the boundaries and also reduced the possibility of choosing a set of parameters for which the vehicle would be uncontrollable.

A photograph of the simulator cockpit is presented in figure 9. The cockpit arrangement, including pilot displays, annunciator lights, switch positions, and controllers, is similar to that of the actual vehicle. Tasks flown and evaluated with the simulator were identical to those in the flight-test program. In addition to the vehicle flight instruments, a two-axis x-y coordinate plotter was used to present longitudinal and lateral position over the ground to the pilot.

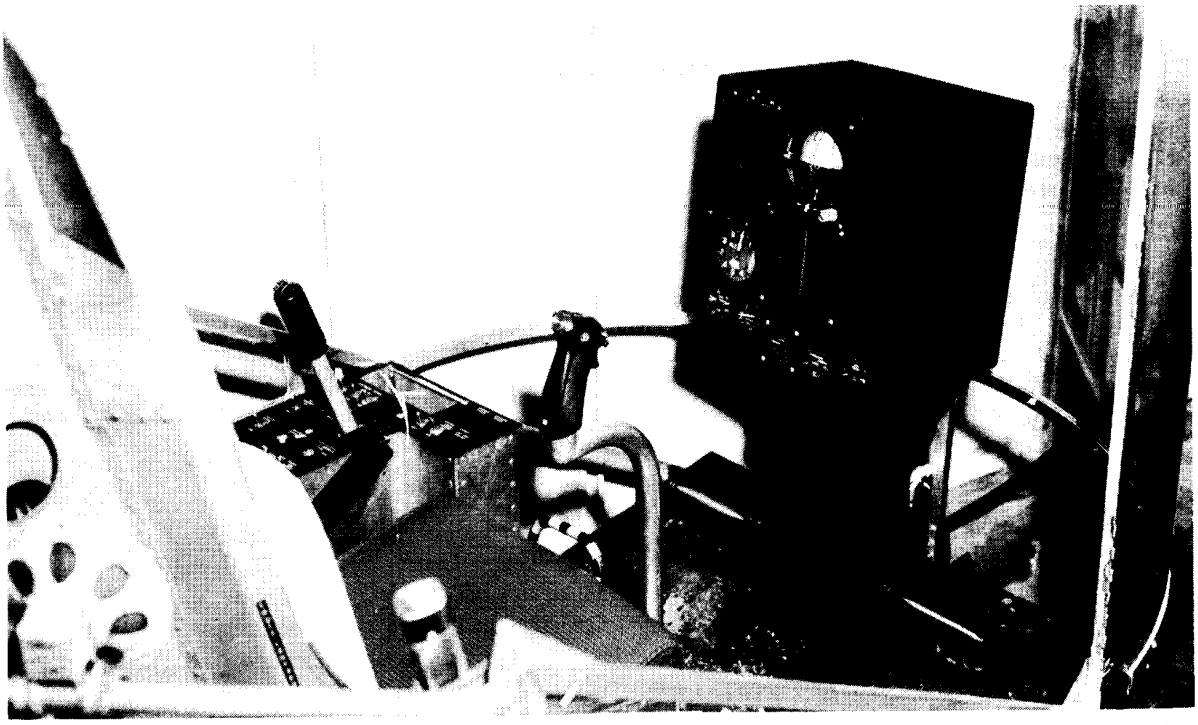

E-10839

Figure 9.– LLRV fixed-base simulator cockpit.

RESULTS AND DISCUSSION

Control Authority

In figure 10 the control boundaries obtained for various control authorities and rate dead band settings about the pitch and roll axes for both VTOL and lunar-simulation operation are presented. These boundaries resulted in pilot ratings of 3.5, as derived from fixed-base simulator tests and based on the rating scale shown in table I. The solid boundary represents VTOL operation and the dashed boundary, lunar simulation. The area between each boundary and the ordinate denotes the particular values and combinations of control authorities and rate dead bands which resulted in pilot ratings better than 3.5. The area outside each boundary denotes the parameter values which resulted in various degrees of unsatisfactory operation or pilot ratings poorer than 3.5. The boundaries were obtained for the longitudinal translation and landing task. The data points in the figure represent the combinations of control authority and rate dead bands that were evaluated with the LLRV, and the numbers adjacent to each symbol represent the pilot rating for that particular condition. The circles represent ratings from the VTOL portion of the flights, and the squares represent ratings from the lunar-simulation portion of the flights.

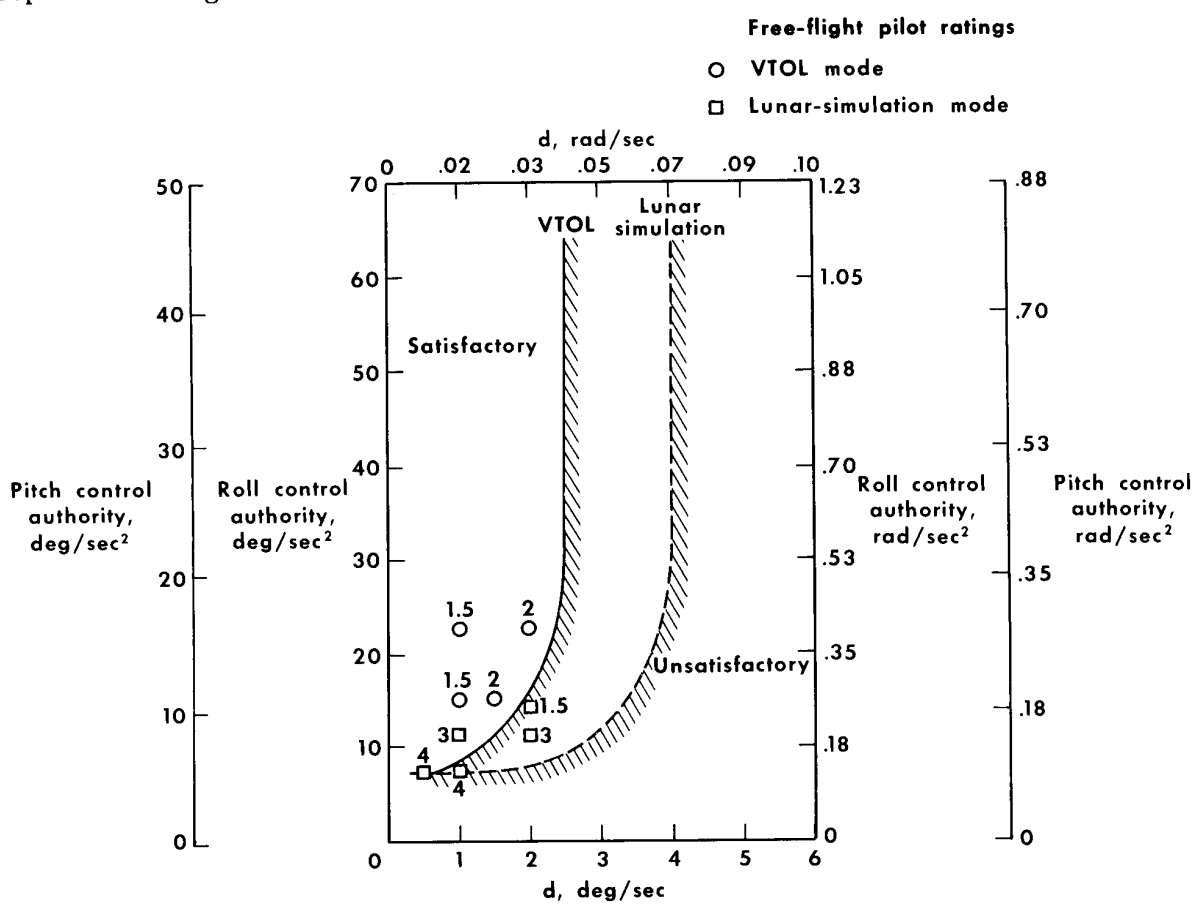

Figure 10.– Comparison of LLRV flight data with fixed-base simulator pitch-roll control authority boundaries for VTOL and lunar-simulation operation. Longitudinal translation and landing task. K = 3 seconds^{-1}.

The most significant item illustrated in figure 10 is the larger area of satisfactory rating experienced with operation in a lunar-gravity environment than with VTOL operation. The dead band (damping) requirements for lunar-simulation operation were considerably reduced at all values of control authority. Maximum satisfactory values of dead band settings were 2.5 deg/sec (0.04 rad/sec) for VTOL operation and approximately 4 deg/sec (0.07 rad/sec) for lunar-simulation operation. As shown in the figure, these values are the upper dead band limits for pitch and roll control authorities greater than 21.5 deg/sec^2 (0.38 rad/sec^2) and 30 deg/sec^2 (0.53 rad/sec^2), respectively. Fixed-base simulator results indicate that for control authorities below these values the damping requirements begin to increase for both VTOL and lunar-simulation operation. The minimum values of control authority below which satisfactory operation was not attainable for any rate dead band setting were on the order of 5 deg/sec^2 (0.09 rad/sec^2) and 7.5 deg/sec^2 (0.13 rad/sec^2) for pitch and roll, respectively. LLRV flights were made at these particular values of control authority and, as shown in the figure, tended to substantiate the lower boundary. These results seem to be in agreement with the six-degree-of-freedom simulator results in reference 8, in which evaluation of a similar type of rate command system indicated that satisfactory control could be experienced with minimum authorities of approximately 8 deg/sec^2 (0.14 rad/sec^2) for both pitch and roll.

It should be emphasized, however, that operation at these low authority levels demands that extremely tight tolerances for extraneous moment disturbances be observed. Flight experience with the LLRV has shown that unbalance moments due to unequal fuel usage from separate storage tanks, aerodynamic disturbances, and thrust misalinement are extremely difficult to alleviate from a normal operational point of view. Pilot ratings of LLRV controllability have been found to deteriorate when vehicle unbalance about a particular axis reaches 20 percent to 25 percent of the control authority. An independent fixed-base simulator study (ref. 9) arrived at optimum handling qualities for unbalance torques less than 15 percent to 20 percent of available control authority, which is in general agreement with LLRV results.

Although the area of satisfactory controllability from the standpoint of control authority and damping was found to be much larger for lunar-simulation operation, the pilots tended to prefer flying in the VTOL mode. The large attitude angles required for translation in the lunar mode by vectoring the lift-rocket thrust were disconcerting to pilots with conventional VTOL and helicopter experience. It is interesting to note that this dislike was not perceived during the fixed-base simulator studies. The pilots did, in fact, reflect the larger satisfactory control region associated with lunar operation by stating a general preference for this mode as opposed to VTOL operation during the fixed-base simulator program. However, it was found that, although the motion cues present during lunar-simulation operation with the LLRV distracted the pilot, motion cues experienced during VTOL operation were extremely beneficial from the control standpoint and were desired by the pilots.

Controller Sensitivity

Pitch and roll control. – The effect of controller sensitivity on the VTOL and lunar-simulation control boundaries is shown in figure 11. The boundaries, which were obtained from fixed-base simulator studies, represent a constant control authority of 10 deg/sec^2 (0.18 rad/sec^2) about the pitch axis and 15 deg/sec^2 (0.26 rad/sec^2) about the roll axis. The solid boundary corresponds to VTOL operation and the dashed

boundary, lunar-simulation operation. The area between each boundary and the ordinate represents values of controller sensitivity and rate dead band that result in pilot ratings less than 3.5. The data points and adjacent numbers represent pilot ratings from actual LLRV flights.

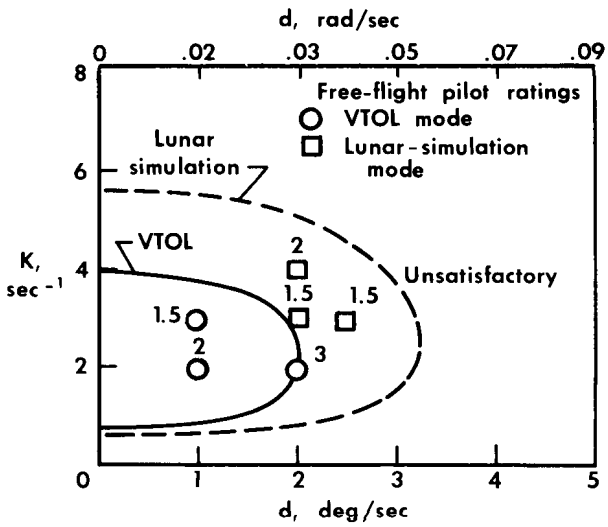

Figure 11.– Comparison of LLRV flight data with fixed-base simulator pitch-roll control sensitivity boundaries for VTOL and lunar-simulation operation. $\ddot{\theta} = 10$ deg/sec^2 (0.18 rad/sec^2); $\ddot{\varphi} = 15$ deg/sec^2 (0.26 rad/sec^2).

Again, the relatively large choice of parameters for lunar-simulation operation as opposed to VTOL operation is denoted by the relative sizes of the satisfactory regions in figure 11. The pilot's willingness to operate with larger rate dead bands during lunar simulation is again shown, as in figure 10, by the difference in maximum rate dead bands. The bottom limits of the two boundaries are similar in figure 11. The upper boundaries for the two modes are quite distinct, however, with the pilot willing to accept a maximum control sensitivity of 5.5 sec^{-1} for lunar simulation as compared with a maximum 4 sec^{-1} for VTOL operation. This seems to be a direct result of the more critical attitude requirement associated with VTOL operation in which vectoring the large jet-engine thrust requires small angles for translation and tends to increase the task of maintaining small attitude angles. For the lunar-simulation maneuver, small attitude angles are tolerable with no significant change in translational velocities, and a higher controller sensitivity is acceptable.

In figure 12, the control sensitivity and rate dead band boundaries delineating satisfactory and unsatisfactory control are shown for several values of control authority about the pitch and roll axes as determined from fixed-base simulator studies. Figure 12(a) represents VTOL operation and figure 12(b), lunar-simulation operation. All the boundaries shown were obtained by using the longitudinal translation and landing task. The data points indicate LLRV flights that were made at the particular condition denoted by the point. The different symbol shapes correspond to distinct values of LLRV control authorities evaluated, as shown in the key. The pilot ratings for each LLRV flight are presented with each data point.

General agreement between the fixed-base simulator boundaries and flight-test results is good. In figure 12(a), all pilot ratings of vehicle controllability except one are better than 3.5 and fall within the specified control-authority boundary. It must be emphasized that, because of the critical nature of the control problem associated with the vehicle, no attempt was made to explore the unsatisfactory areas indicated by each boundary.

In figure 12(b), the willingness of the pilot to accept an increased sensitivity and less damping is again indicated by the relatively larger satisfactory areas denoted by each lunar-simulation boundary as compared to VTOL operation in figure 12(a).

Boundary	Pilot rating symbol	Control authority $\ddot{\theta}$ deg/sec^2 (rad/sec^2)	Control authority $\ddot{\varphi}$ deg/sec^2 (rad/sec^2)
A	–	47.5 (.83)	68 (1.2)
B	–	21 (.37)	30 (.53)
–	○	16 (.28)	22.5 (.39)
C	□	10 (.18)	15 (.26)
D	–	5 (.09)	7.5 (.13)

Boundary	Pilot rating symbol	Control authority $\ddot{\theta}$ deg/sec^2 (rad/sec^2)	Control authority $\ddot{\varphi}$ deg/sec^2 (rad/sec^2)
A	–	47.5 (.83)	68 (1.2)
B	–	21 (.37)	30 (.53)
C	△	10 (.18)	15 (.26)
–	○	8 (.14)	11 (.19)
D	□	5 (.09)	7.5 (.13)

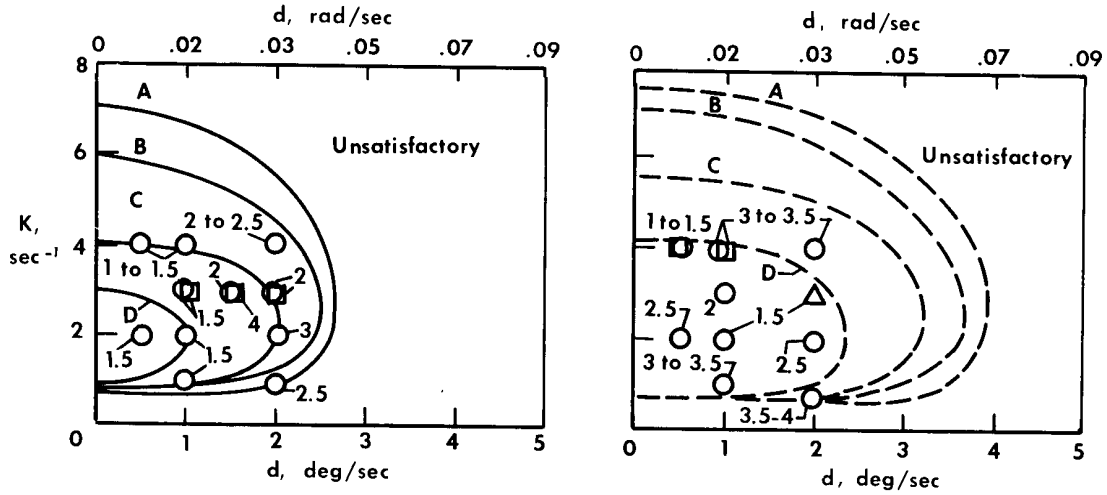

(a) VTOL mode.

(b) Lunar-simulation mode.

Figure 12.– Effect of control authority on pitch and roll control sensitivity boundaries. Longitudinal landing and translation task.

Yaw control. – Experience with both the fixed-base simulator and the LLRV indicates that the longitudinal-translation and landing-task investigation places a minimum requirement level on the parameters selected for yaw control. Results have shown that satisfactory control can be accomplished even without rate damping, as long as sufficient control authority is provided about the yaw axis to override disturbing torques. Because the problem of selecting yaw-control parameters seems to be modest compared to pitch and roll control, the control requirements about the yaw axis were not investigated to as great a degree as the pitch and roll requirements.

Values of rate dead band and control sensitivity resulting in satisfactory yaw controllability are presented in figure 13. The data points represent the parameter evaluated during actual flight tests. The numbers adjacent to the points are actual pilot ratings. The control task was the longitudinal translation and landing maneuver. The data points correspond to a yaw-control authority of 7.5 deg/sec^2 (0.13 rad/sec^2).

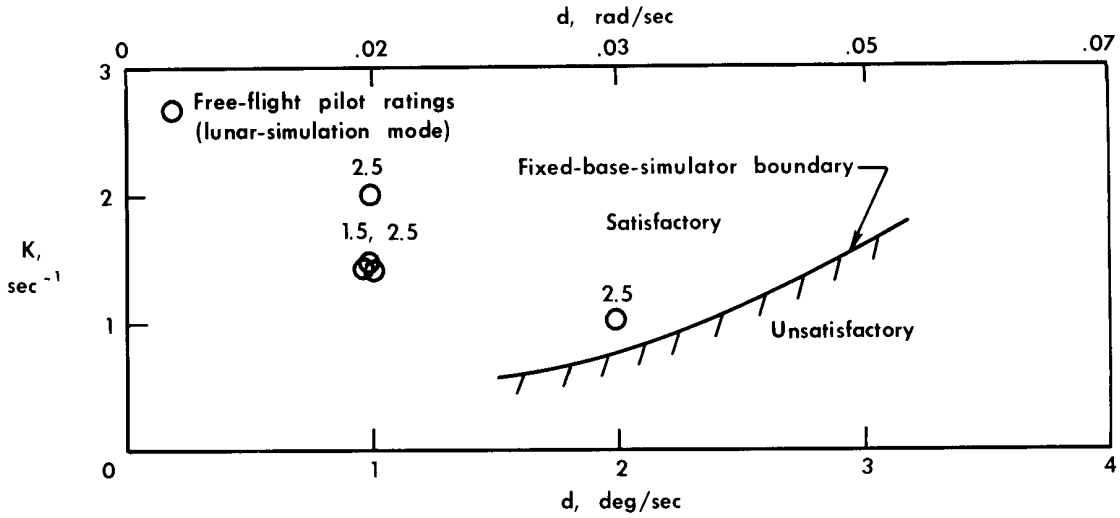

Figure 13.– Pilot ratings of yaw control sensitivity and rate dead band for the longitudinal translation and landing task. Yaw control authority = 7.5 deg/sec^2 (0.13 rad/sec^2).

Control Harmony

During both the LLRV fixed-base simulator and flight-test programs, it was noted that the pilots would usually assign the same numerical ratings to each axis, even though the control authority about individual axes differed significantly at times. This characteristic was noted particularly during several LLRV flights in which operation in the lunar-simulation mode was uncontrollable about the roll axis because of a lateral center-of-gravity shift. Although the pitch and yaw axes were not affected, a pilot rating of unsatisfactory was assigned to all three axes. The effect of control harmony and interaxis coupling on pilot ratings is discussed in detail in reference 10. Simulator studies in reference 10 show that where conditions about one control axis are deteriorated, with satisfactory control about the other axis remaining fixed, the pilot ratings for all axes deteriorate.

Lateral balance of the LLRV has been a severe problem that has affected control harmony and pilot ratings, particularly during lunar-simulation operation at low control authorities. Since the rockets used to correct for unbalance moments are also used to provide pilot inputs, the obvious effect is to reduce the control authority available to the pilot for normal attitude corrections. Another effect has been noted, however, which results from the logic arrangement of the LLRV attitude control system.

The LLRV attitude-rocket control logic is arranged so that two rockets are operated simultaneously about a given axis to provide control (fig. 6). The pitch and roll rockets form an additive couple about the particular axis being controlled and a subtractive couple about the axis for which no motion is desired. When a combined pitch-roll input is applied to the system, only one rocket is operating, which causes motion about both axes at one-half the normal authority. With this arrangement, it is possible for the pilot to experience a false indication of pitch and roll coupling resulting from an unbalanced vehicle.

The effect of unbalance and rocket logic is illustrated in figure 14, a time history of a portion of an actual LLRV flight in which a large roll-left unbalance occurred as the result of unequal propellant consumption from the side-mounted hydrogen-peroxide storage tanks. The figure shows pitch and roll stick position and angular rate and attitude-rocket thrust as a function of time. The firing logic for the attitude rockets was shown in figure 6. A nose-heavy condition also existed, and the resultant motion due to the lateral and longitudinal unbalance was a tendency for the vehicle to pitch down and roll left. It can be seen in figure 14 that the C_S attitude rocket was being fired almost continuously by the damper to counteract the unbalance. (The C_S rocket firing singularly results in both a roll-right and pitch-up control moment.)

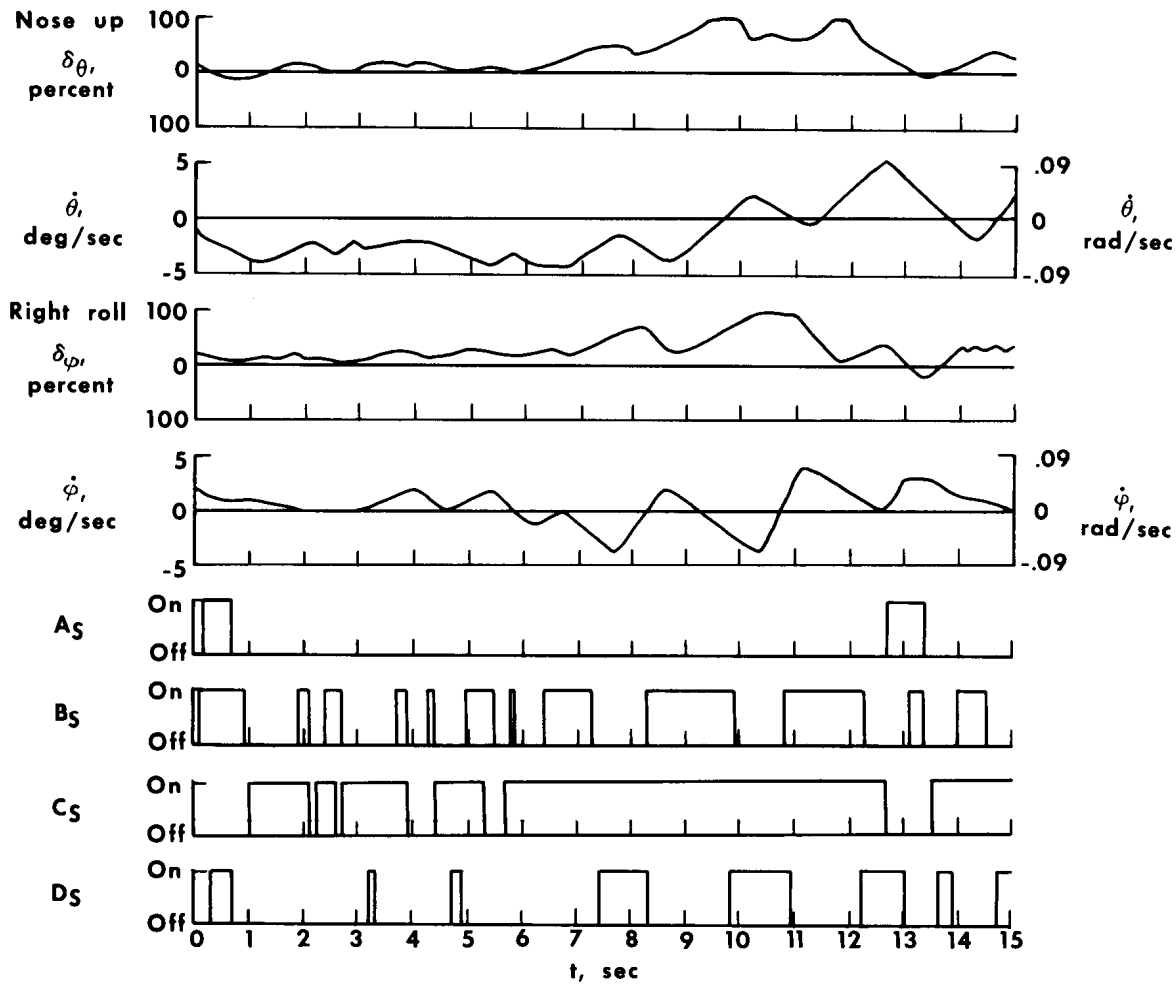

Figure 14.– Time history showing effect of unbalance and rocket logic on LLRV controllability. Control authority: pitch, 5 deg/sec^2 (0.09 rad/sec^2), roll, 7.5 deg/sec^2 (0.13 rad/sec^2); $d_\theta = d_\varphi = 1$ deg/sec (0.02 rad/sec); $K_\theta = K_\varphi = 4$ sec^{-1}.

At t = 6 seconds (fig. 14), a pitch-up input was initiated by the pilot. At this time, the C_S rocket was firing singularly to compensate for both the pitch and roll unbalance. At t = 6.4 seconds, the B_S rocket was fired, as a result of the pitch-up pilot command, and coupled with the C_S rocket to provide a pure pitch-up control moment. This canceled the roll-right moment provided by the C_S rocket. The

result was that the vehicle not only began to rotate nose up but also rolled to the left. The pilot then applied a roll-right stick input at $t = 7$ seconds, which caused the B_S rocket to shut off at $t = 7.3$ seconds. The D_S rocket then fired and coupled with the C_S rocket to provide a pure roll-right moment.

With proper motion thus restored to the vehicle, the pilot again initiated a nose-up command and began to return the control stick to a neutral position for roll at $t = 8.2$ seconds. At $t = 8.3$ seconds the D_S rocket was shut off and the B_S rocket fired, again coupling with the C_S rocket, canceling the roll-right moment and providing a pure pitch-up moment. As in the previous instance, the vehicle began a nose-up rotation in response to the B_S and C_S rocket couple and rolled left as a result of lateral unbalance. As in the previous case, roll-left vehicle motion resulted from pitch-up stick deflections. After the pilot applied corrective inputs, this effect was again experienced at $t = 11$ seconds.

The pilot, unable to judge whether the correct attitude rockets are firing in correspondence to a particular stick deflection, relies on the relative motion of the vehicle with respect to the control stick for this information. The pilot stated that, in this particular instance, the effect was that of commanding pitch-up vehicle motion but receiving roll-left motion. The pilot's sensation was that a malfunction had occurred in the logic circuitry associated with the control system. This effect was not encountered at pitch and roll control authorities above 10 deg/sec^2 (0.18 rad/sec^2) even for a large vehicle unbalance. The higher angular accelerations seem to be effective in masking out the undesirable vehicle motions. For low control authorities, however, vehicle angular accelerations are such that pilots are able to detect the cross-coupling effect.

The significance of the problem is that any externally applied disturbing moment can result in a dynamically unstable vehicle at low values of control authority. In figure 14 the combination of low authority, vehicle unbalance, and attitude-rocket logic results in pilot-induced oscillations about the pitch and roll axes. Divergent characteristics can be noted in the motions about both axes. If the pilot had not been able to select a higher control authority, the results could have been catastrophic.

Controllability at Large Attitudes

Previous studies of VTOL handling qualities have indicated that specific control tasks should not be the sole criterion in evaluating VTOL controllability (ref. 4). In order to investigate controllability of the LLRV at attitudes and translational velocities greater than those required to accomplish the longitudinal translation and landing task, a large-angle task (discussed on page 9) was also evaluated during lunar-simulation operation.

LLRV controllability at large attitudes during lunar-simulation operation was not found to differ significantly from the results shown in figure 12(b) for control authorities greater than 10 deg/sec^2 (0.18 rad/sec^2) and 15 deg/sec^2 (0.26 rad/sec^2) about pitch and roll, respectively. For authorities less than these values, however, experience shows that unsatisfactory controllability can result with the large-angle

evaluation task at parameter settings that exhibited satisfactory controllability characteristics with the less demanding longitudinal translation and landing task.

This deterioration in LLRV controllability at large attitudes and translational velocities for low control authorities is a direct result of the balance and control-logic problem discussed in the preceding section. The higher translational velocities result in aerodynamic moments acting on the vehicle in the same manner as any unbalancing moment. The large vehicle attitudes require large pilot commands which, when coupled with the low control authority and rocket logic, result in interaxis coupling that is undesirable from a piloting viewpoint.

Limit-Cycle Operation

As with any control system that uses nonlinear elements, it was necessary that the nonlinear response and limit-cycle operation of the LLRV attitude control system be adequately defined for the various parameters to be investigated during the flight-test program. It was felt that control parameters should be selected during the initial LLRV flights that would result in stable vehicle response with no limit-cycling. It was necessary, then, to define the limit-cycle boundary and insure that the selected parameters would be well within a stable region.

The describing-function technique of nonlinear system analysis was used to determine the limit-cycle characteristics of the LLRV rate command system. The technique, which is similar to that outlined in references 11 and 12, is presented in the appendix.

Results of the LLRV limit-cycle analysis are shown in figure 15, in which the limit-cycle boundary is plotted as a function of rate dead band and control authority about the pitch and roll axes. The area above the boundary line denotes stable vehicle response, and the area below the boundary represents parameter combinations which result in limit-cycle operation. The data points correspond to parameter values that have been evaluated on the LLRV. The solid symbols represent actual LLRV flights; whereas, the open symbols represent LLRV ground tests in which the vehicle was mounted on a pivoting fixture and allowed the freedom of angular rotation (ref. 6). The squares indicate the occurrence of a limit-cycle oscillation at the particular condition represented; whereas, the circles indicate that no limit cycle occurred at that condition.

Agreement between actual and analytical results has, in general, been good. In a small area close to the boundary line in figure 15 there is some question regarding the occurrence or nonoccurrence of oscillations. This area results from the fact that the describing-function technique used in the theoretical analysis makes use of an approximation of the nonlinear element characteristics, thus allowing the characteristics to be treated in a linear fashion.

Pilots who have experienced the limit cycling of the rate command system during flight did not notice a deteriorating effect on vehicle controllability. The frequency and amplitudes of the limit cycles were not objectionable from this standpoint. However, the noise created by the attitude rockets firing at the limit-cycle frequency (approximately 2 cps) and instrument-panel vibrations were distracting to pilots, particularly at high values of control authority.

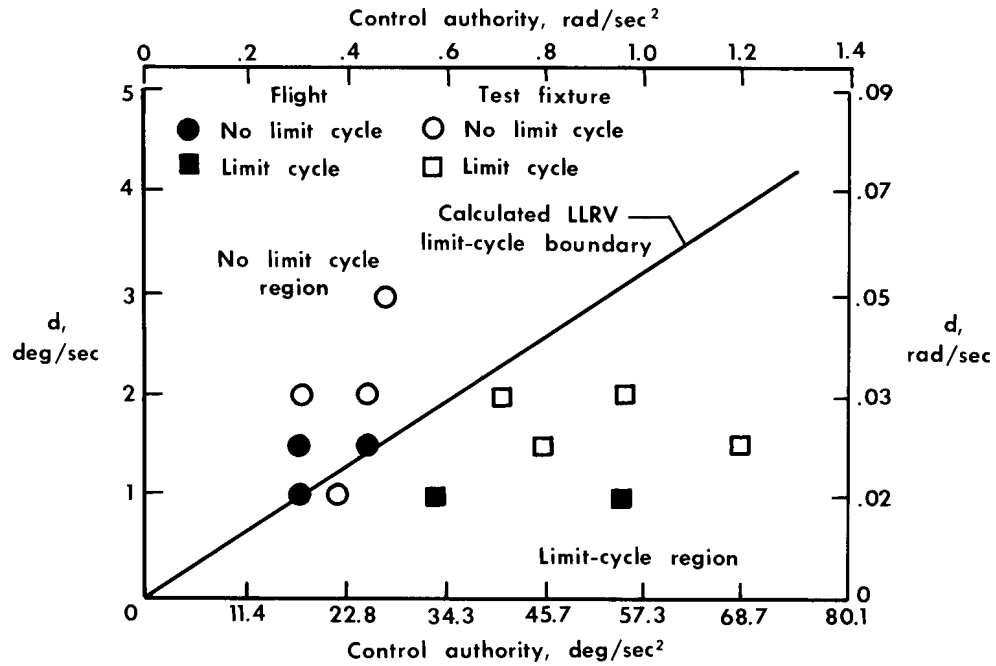

Figure 15.– LLRV rate command system limit-cycle boundary.

In figure 16 the LLRV rate command system pitch and roll limit-cycle amplitude characteristics determined from analog-simulator results are shown as a function of rate dead band setting. The limit-cycle response for several control authorities was investigated. Specific control authorities investigated are shown in figures 16(a) and 16(b).

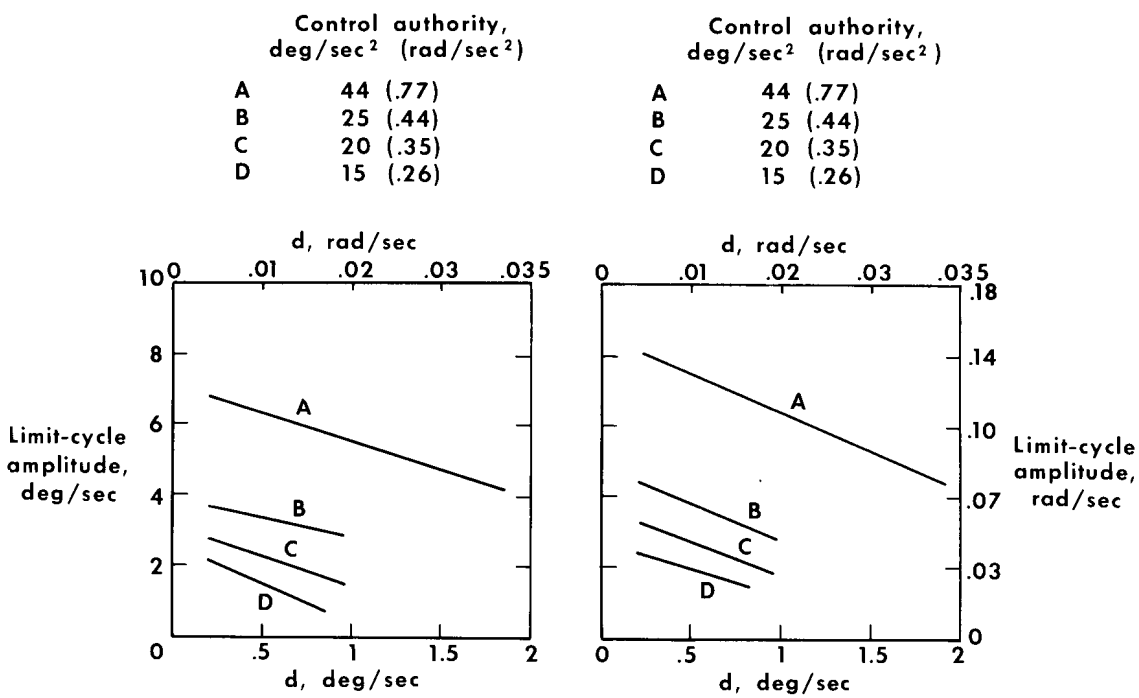

(a) Pitch. (b) Roll.

Figure 16.– LLRV rate command system limit-cycle characteristics determined from analog-simulator studies.

Attitude-Rocket Propellant Consumption

During the LLRV fixed-base simulator evaluation of the rate command system, the attitude-rocket firing pulses were integrated to provide total impulse over the time required to complete the longitudinal translation and landing maneuver. The rate of propellant consumption required to complete the task was then computed on the basis of a specific impulse of 120 seconds for the hydrogen-peroxide attitude rockets, and an average consumption rate was calculated.

The effects of stick sensitivity, rate dead band, and rocket thrust on the propellant requirements for the task involved are presented in figures 17 to 20 for VTOL and lunar-simulation operation. Each of the figures corresponds to a specific value of attitude-rocket thrust or control authority. The curves relate to distinct values of control sensitivity. For each value, the rate of attitude-rocket propellant consumption is shown as a function of rate dead band setting.

The results of this investigation indicate that for all control authorities and sensitivities evaluated the minimum propellant consumption always occurs at approximately the same rate dead band setting. This is indicated by the troughs which occur in the propellant-usage curves shown in figures 17 to 20. The minimum value of propellant consumption appears to occur always between rate dead bands of 1.5 deg/sec (0.03 rad/sec) to 2.5 deg/sec (0.04 rad/sec) and is independent of the parameters selected. The point of minimum fuel usage is also more sharply defined at the lower level of control authority (fig. 17) than the minimum points for the higher-authority curves (fig. 20). This characteristic is believed to result from the fact that the increase in propellant usage at the wider dead band settings is brought about by the decrease in closed-loop stability. As the closed-loop stability is diminished, a greater number of control inputs are required by the pilot for vehicle attitude correction, which results in inefficient operation. As the dead band settings are widened, the control system is also transformed into an on-off acceleration command mode of operation. Previous studies (refs. 13 and 14) have shown that this type of control is somewhat satisfactory for relatively large control authorities but results in unsatisfactory control at low values of control authority. Unsatisfactory control at low authorities is a contributing factor, resulting in the slower rise in propellant consumption for wider dead band settings experienced with large values of control authority (fig. 20) than for smaller control authorities (fig. 17). The increase in propellant consumption at the smaller dead band setting in figures 17 to 20 is caused by increased damping supplied by the attitude rockets and limit-cycle operation.

Comparison of fuel usage for conventional VTOL operation and lunar-simulation operation indicates no significant difference at the lower values of control sensitivity. There is an increase in propellant consumption with VTOL operation at the higher control sensitivities that is not reflected in the lunar-simulation operation. This is particularly true at the higher control authorities (figs. 19 and 20).

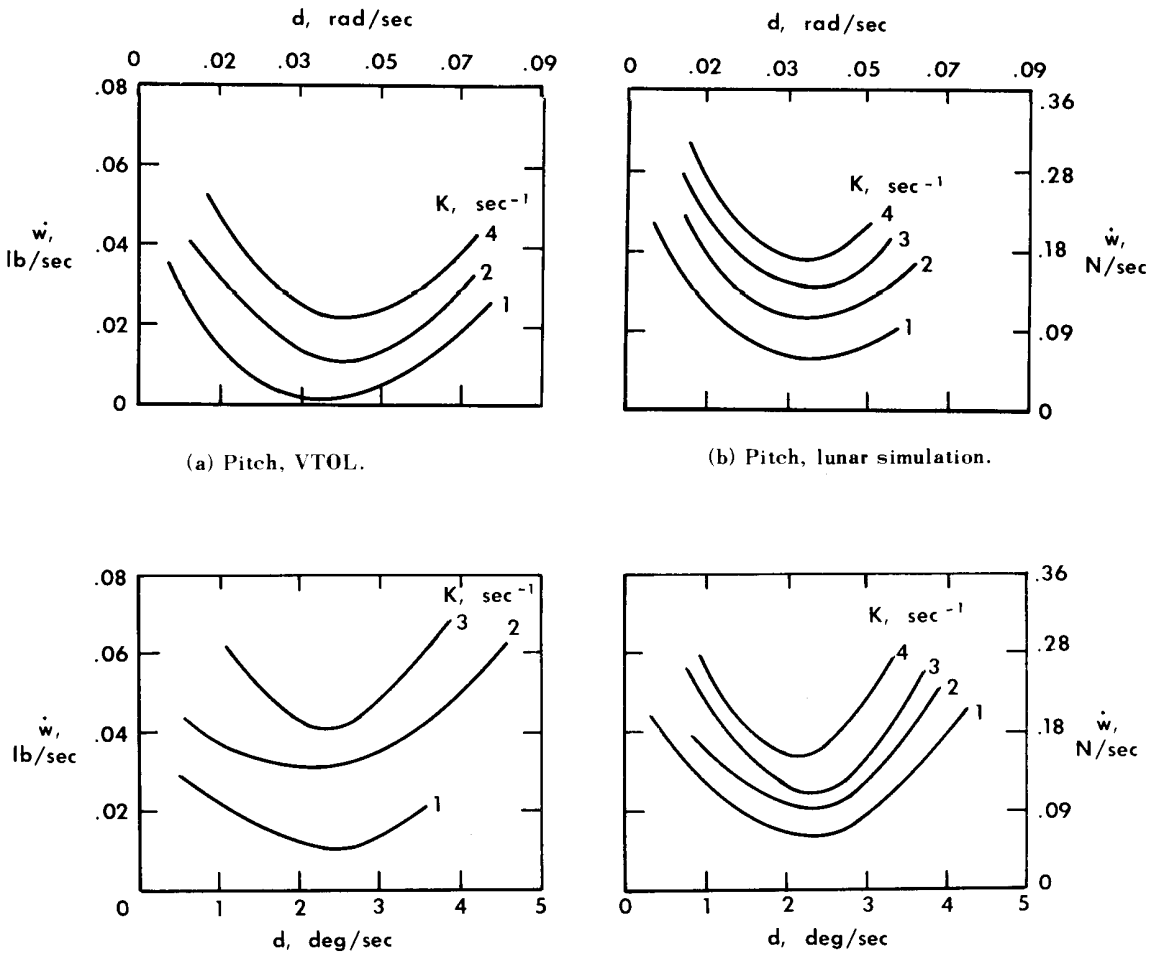

Figure 17.—Effect of controller sensitivity on rate command system propellant consumption. $\ddot{\theta}=5$ deg/sec^2 (0.09 rad/sec^2); $\ddot{\varphi}=7$ deg/sec^2 (0.12 rad/sec^2).

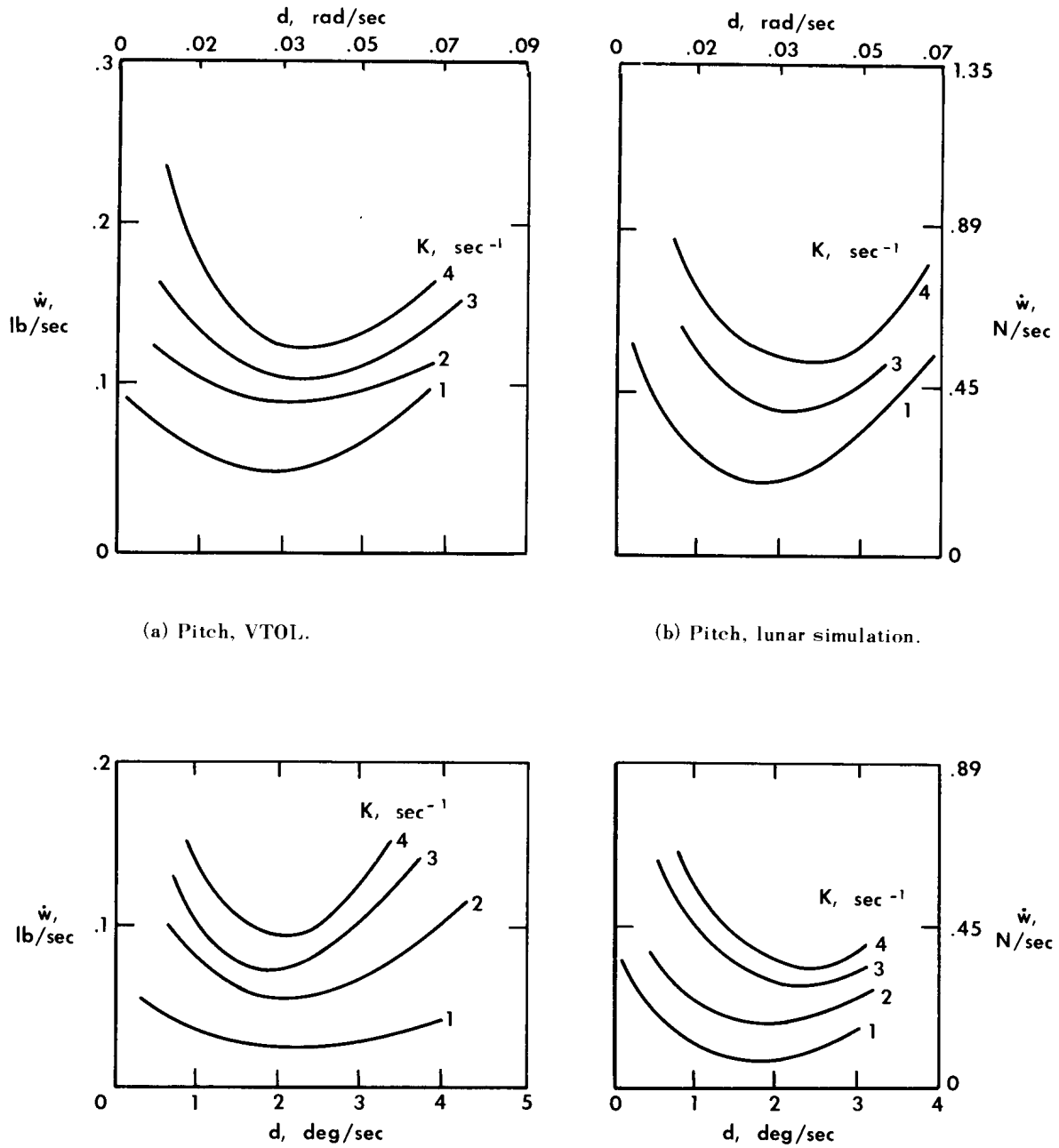

(a) Pitch, VTOL.

(b) Pitch, lunar simulation.

(c) Roll, VTOL.

(d) Roll, lunar simulation.

Figure 18.– Effect of controller sensitivity on rate command system propellant consumption. $\dot{\theta} = 10$ deg/sec^2 (0.18 rad/sec^2); $\ddot{\varphi} = 14$ deg/sec^2 (0.24 rad/sec^2).

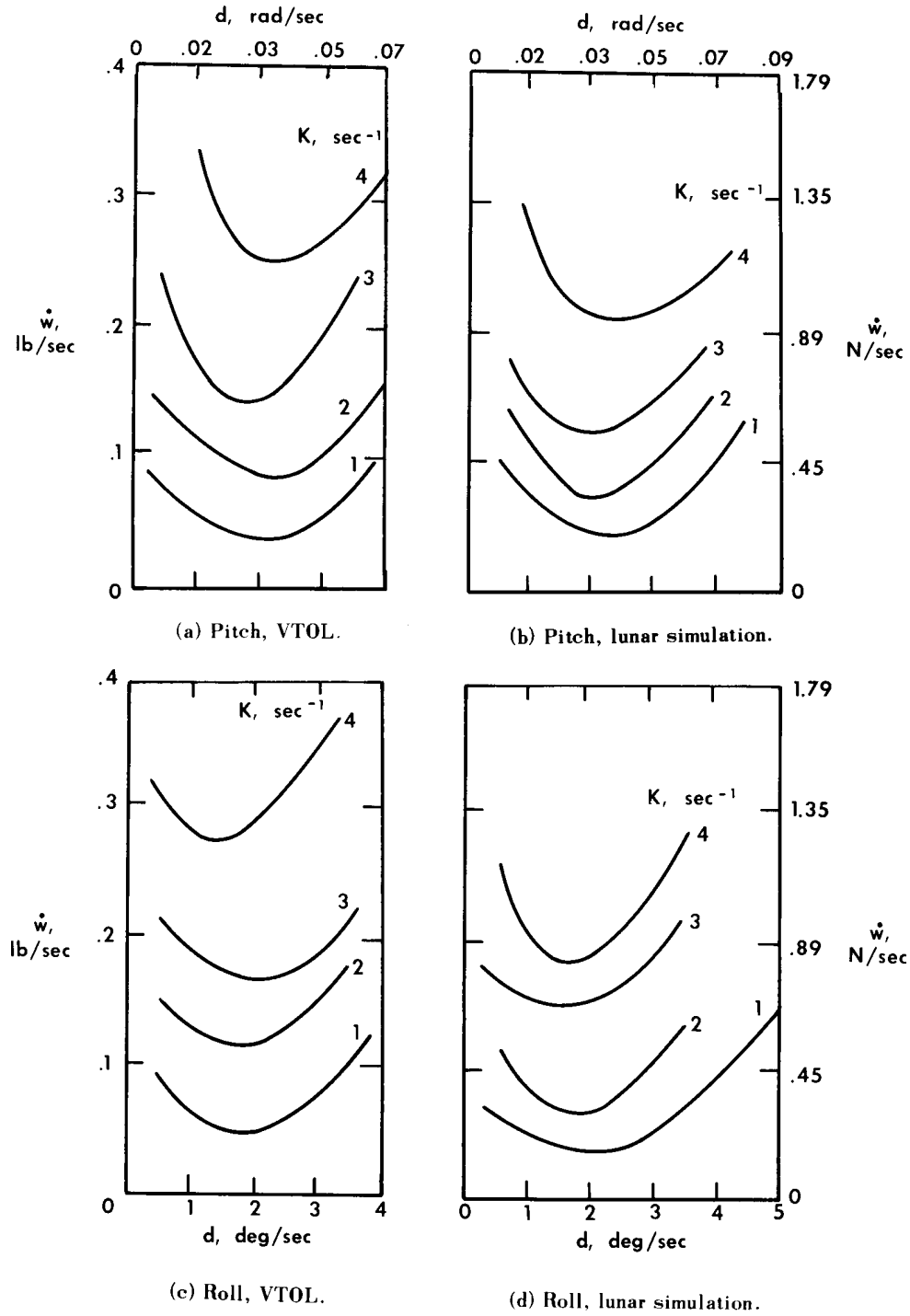

Figure 19.—Effect of controller sensitivity on rate command system propellant consumption. $\dot{\theta} = 15$ deg/sec^2 (0.26 rad/sec^2); $\dot{\varphi} = 21$ deg/sec^2 (0.37 rad/sec^2).

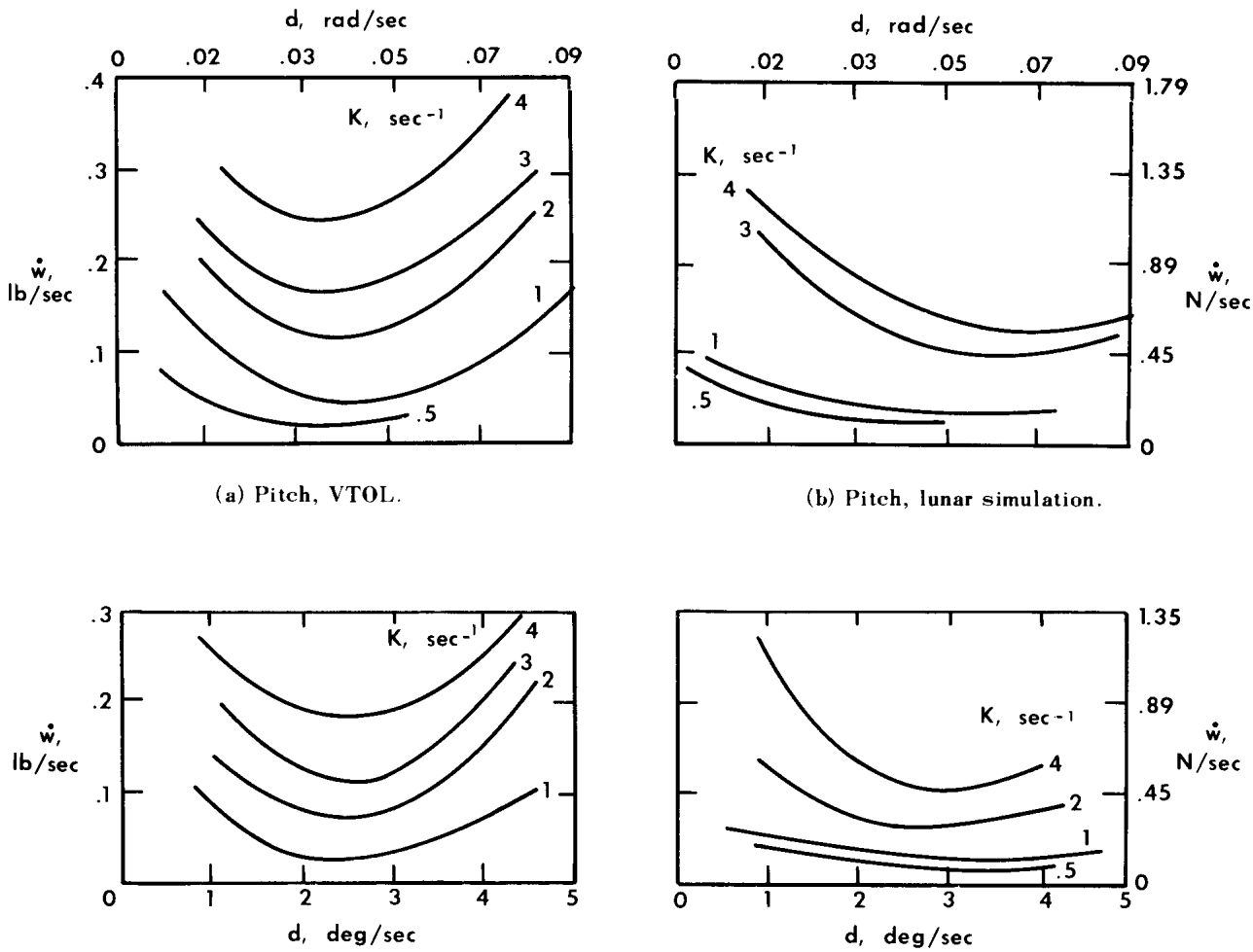

(a) Pitch, VTOL.

(b) Pitch, lunar simulation.

(c) Roll, VTOL.

(d) Roll, lunar simulation.

Figure 20.– Effect of controller sensitivity on rate command system propellant consumption. $\ddot{\theta} = 45$ deg/sec^2 (0.79 rad/sec^2); $\ddot{\varphi} = 63$ deg/sec^2 (1.1 rad/sec^2).

In figures 21 and 22 fixed-base simulator fuel-usage data are compared with experience during actual flight tests with the LLRV. The data points show the attitude-rocket fuel consumption about a particular axis while the longitudinal translation and landing task was being performed. The control sensitivities corresponding to each data point are shown in the keys. The data in figure 21 were obtained from VTOL operation with the LLRV at pitch and roll control authorities of 15 deg/sec^2 (0.26 rad/sec^2) and 21 deg/sec^2 (0.37 rad/sec^2), respectively. Figure 22 presents data obtained from lunar-simulation flights at control authorities of 10 deg/sec^2 (0.18 rad/sec^2) and 14 deg/sec^2 (0.24 rad/sec^2) for pitch and roll.

The flight data are in general agreement with the simulator results. A higher rate of fuel consumption was experienced with higher control sensitivities and tighter dead bands, with minimum rates occurring around a dead band of 2 deg/sec (0.03 rad/sec). The actual values of fuel consumption agree favorably with simulator results except for lunar-simulation control about the roll axis at the low control authority. The discrepancy is a result of lateral unbalance conditions experienced with the vehicle but not included in the simulation program.

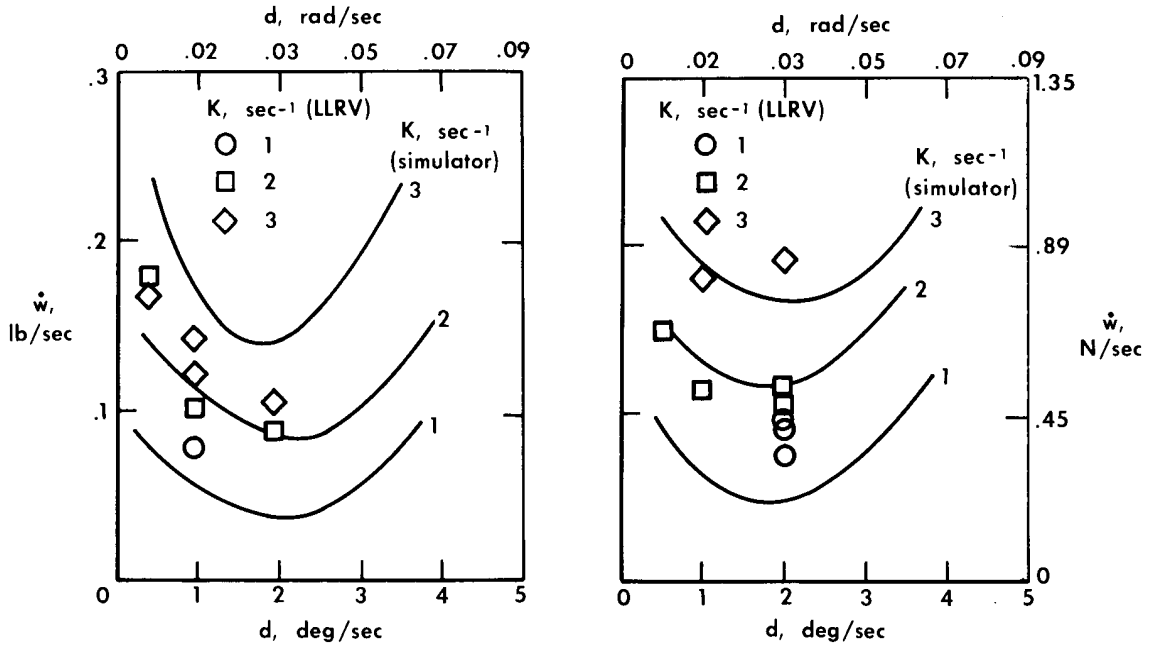

(a) Pitch. (b) Roll.

Figure 21.– Comparison of actual LLRV-VTOL attitude-rocket propellant consumption from flight-test data with fixed-base simulator results. $\ddot{\theta} = 15$ deg/sec^2 (0.26 rad/sec^2); $\ddot{\varphi} = 21$ deg/sec^2 (0.37 rad/sec^2).

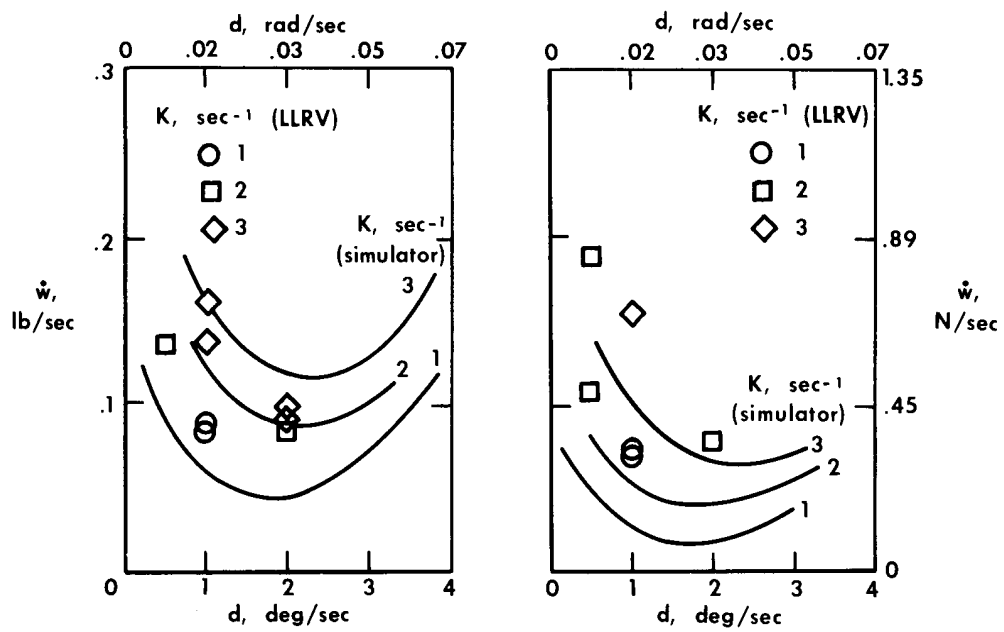

(a) Pitch. (b) Roll.

Figure 22.– Comparison of LLRV lunar-simulation attitude-rocket propellant consumption from flight-test data with fixed-base simulator results. $\ddot{\theta} = 10$ deg/sec^2 (0.18 rad/sec^2); $\ddot{\varphi} = 14$ deg/sec^2 (0.24 rad/sec^2).

Comparison of On-Off and Proportional VTOL Attitude Control

The primary advantage of an on-off type of attitude control system over conventional proportional control is that control torque required for damping does not reduce the control authority available to the pilot. This feature allows satisfactory operation at greatly reduced control torques and, consequently, less fuel consumption for systems using attitude-rocket thrusters.

In figure 23 LLRV data are compared with flight data from several VTOL vehicles which utilize various techniques for generating proportional attitude control. The control parameters and pilot ratings for these vehicles were obtained from reference 10.

In order to correlate the proportional systems with the LLRV on-off system, the comparative damping of each vehicle evaluated, given its maximum control torque, was computed for each rate dead band setting by using the following relationship:

$$\frac{\ddot{\theta}}{d} = \text{Comparative damping, } \frac{1}{\text{sec}}$$

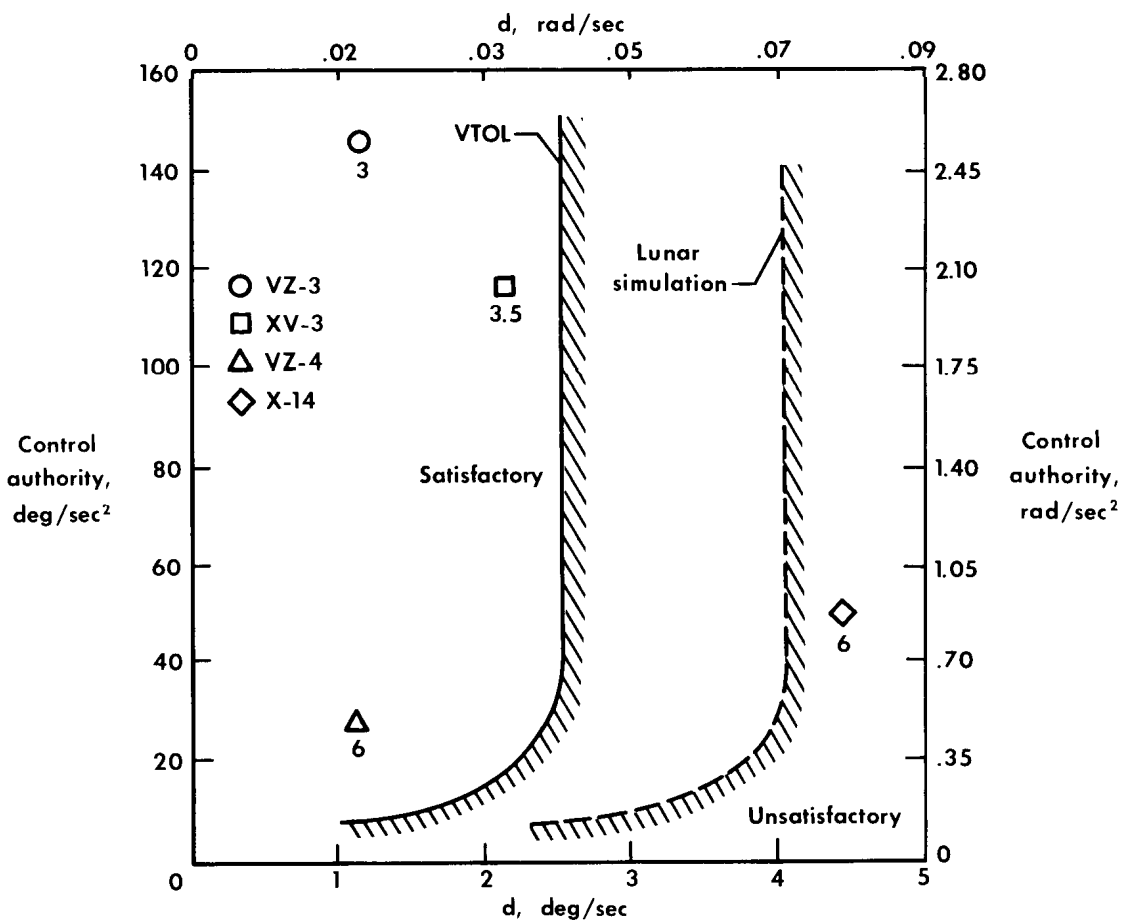

Figure 23.– Comparison of LLRV control boundaries with other VTOL flight data.

This relationship permits a rate dead band to be selected for each of the proportional control vehicles considered, which would result in comparative damping if applied to the LLRV system. The basic difference between the two types of systems may then be considered primarily as the technique of mechanization.

The large values of control authority required by proportional VTOL attitude control systems for satisfactory control, as compared to the LLRV on-off system, are indicated by the satisfactory pilot ratings of VZ-3 and XV-3 controllability experienced with the VTOL vehicles. The damping levels for these two vehicles fall within the specified boundary determined from LLRV experience. The VZ-4 experience, however, shows that, even though a significant level of damping is maintained with proportional systems, the minimum control-authority boundary for satisfactory controllability is significantly higher than that experienced with the LLRV system.

Similar results that indicate the large difference between proportional and on-off system control-authority requirements are discussed in reference 8.

CONCLUSIONS

A flight-investigation of an on-off rate command system for the control of a free-flight lunar-landing research vehicle resulted in the following conclusions:

1. The rate command control boundary associated with vehicle attitude control in a lunar-gravity environment can be expanded from that experienced in conventional VTOL operation to include less damping, lower control authorities, and higher controller sensitivities. Satisfactory LLRV attitude control was attained at pitch and roll control authorities as low as 5 deg/sec^2 (0.09 rad/sec^2) and 7.5 deg/sec^2 (0.13 rad/sec^2), respectively.

2. Large vehicle attitudes and long lead times are required for translation maneuvers in the lunar-simulation mode in comparison to smaller attitude changes and shorter lead times required for the same response in the VTOL mode. This lead time is initially distracting to pilots and results in a preference for conventional VTOL operation rather than lunar simulation. This effect disappears as pilots become more familiar with lunar-simulation operation.

3. Disturbing moments and low values of control authority can result in pilot-induced instabilities about both the pitch and roll axis as a result of the control-logic arrangement of the LLRV. For this reason, the degree to which the disturbing moments can be controlled is the limiting factor in establishing the minimum level of control authority for satisfactory operation.

4. Limit-cycle oscillations experienced by pilots during LLRV operation did not deteriorate vehicle controllability. The oscillations were distracting to pilots, however, at the higher values of control authorities investigated.

5. Attitude-rocket propellant consumption was minimized between rate dead band settings of 1.5 deg/sec (0.03 rad/sec) and 2.5 deg/sec (0.04 rad/sec) for any combination of control authority and controller sensitivity.

Flight Research Center,
National Aeronautics and Space Administration,
Edwards, Calif., October 28, 1966.
924-23-21-13-24

APPENDIX

ANALYSIS OF LLRV RATE COMMAND ATTITUDE-CONTROL-SYSTEM LIMIT-CYCLE CHARACTERISTICS

A block diagram of the LLRV rate command attitude control system is shown in figure 24. The linear components incorporated in the analysis are represented in transfer-function form. The filter network shown is a simple first-order lag designed to attenuate structural vibrations sensed by the rate gyros and fed back into the system. The nonlinear elements include an on-off relay function, with dead zone and hysteresis, and transport delay e^{-st}. The transport delay represents the delay time of the solenoid propellant valve and propellant flow lags. The attitude rockets are represented by a simple first-order lag determined from experimental tests performed on similar hydrogen-peroxide control rockets (ref. 13). The vehicle dynamics are represented by the general control-moment equation about one axis with zero aerodynamic contributions.

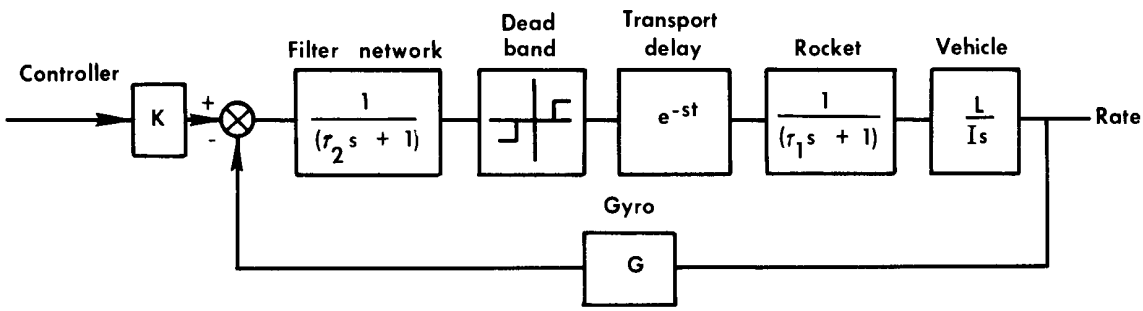

Figure 24.– Block diagram of LLRV rate command attitude control system.

The actual rate gyros used in the system have a natural frequency of 144 rad/sec and a damping ratio of 0.3 to 0.5. The dynamic response of the gyro element is considered to be negligible in this analysis in order to simplify the calculation. As will be shown later, this simplification is not restrictive since the dynamic contribution of the rate-gyro response is small in the area to be investigated.

In using the describing-function technique of nonlinear control systems analysis, the system is generally separated into linear and nonlinear components, as shown in figure 25. In this figure, the linear elements are represented by the G(s) block, where

$$G(s) = \frac{e^{-st}GL}{Is(1 + \tau_1 s)(\tau_2 s + 1)} \tag{1}$$

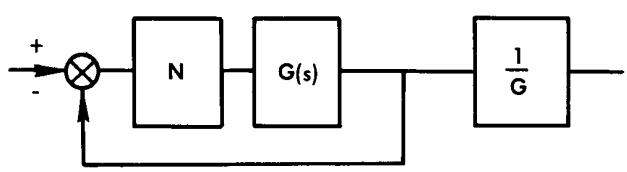

Figure 25.– Separation of attitude control system into linear and nonlinear components.

As seen in equation (1), the transport delay represented by e^{-st} is included in the linear portion of the system. This differs from the procedure outlined in reference 11 in which the transport delay is included in the nonlinear portion but, as shown later, greatly simplifies the analysis.

First, consider the case in which the nonlinear element N, shown in figure 25, is an on-off function with variable dead zone and zero hysteresis. The describing function for this type of nonlinearity is derived in reference 12 as

$$N = \frac{4Y}{\pi X}\sqrt{1 - R^2}\,\angle 0^\circ \tag{2}$$

where

$$R = \frac{d}{2X}$$

As can be seen from this equation, only the gain of the system is affected by this type of nonlinearity; the phase-angle contribution is zero.

In order for a steady-state limit-cycle oscillation to be maintained in a system, it is necessary that the frequency be such that a total phase shift of 180° (3.14 rad) occur when the system gain is unity. Therefore

$$N\,G(s) = -1 \tag{3}$$

and

$$G(s) = -\frac{1}{N} \tag{4}$$

By substituting equation (1) for G(s) and equation (2) for N into equations (3) and (4)

$$\frac{e^{-st}GL}{Is\,(1 + \tau_1 s)\,(\tau_2 s + 1)} = \frac{-\pi X}{4Y\sqrt{1 - R^2}} \tag{5}$$

The value of ω that satisfied the relationship in equation (5) can be determined from the intersection of the gain and phase-angle plots of the G(s) and $-\frac{1}{N}$ equations (eqs. (1) and (2), respectively). In figure 26, the gain-phase plots of the G(s) and $-\frac{1}{N}$ functions are presented for a value of $G\frac{L}{I} = 1$. For small values of ω the G(s) curve follows the 90° (1.57 rad) phase line and, for increasing ω, curves inward and crosses the 180° (3.14 rad) line at $\omega = 13.5$ rad/sec. Since the $-\frac{1}{N}$ curve is not a function of ω, the curve follows the 180° (3.14 rad) line, with each point representing various values of d and X. The intersection of the G(s) curve, therefore, with the 180° (3.14 rad) phase line is the limit-cycle frequency which satisfies equation (5). The limit-cycle frequency for $t = 0.04$ second is 13.5 rad/sec.

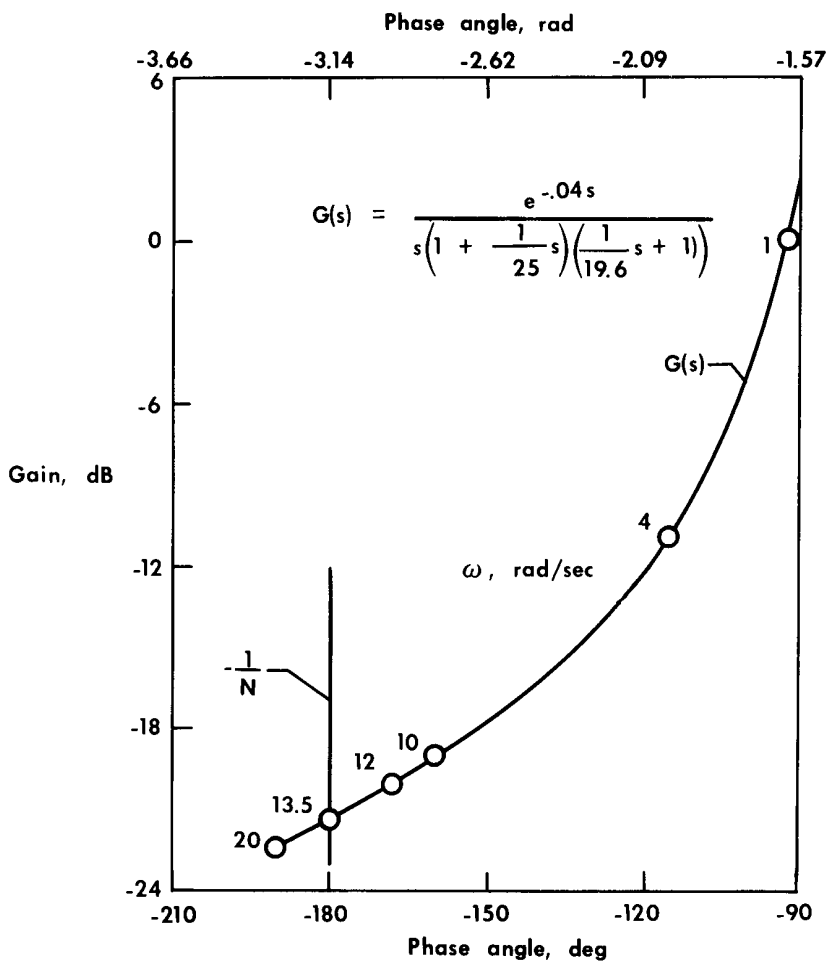

Figure 26.– Gain-phase plot of linear transfer function. $G\frac{L}{I} = 1$.

As noted in figure 26, for this type of nonlinearity, i.e., relay with variable dead zone and no hysteresis, the limit-cycle frequency is a function only of the linear G(s) phase angle. At the intersection of the G(s) and $-\frac{1}{N}$ curves

$$\frac{1}{N} = 21.5 \text{ dB} \tag{6}$$

or

$$N = 11.79 \tag{7}$$

By setting $Y = 1$ in equation (2) and solving for d as a function of X

$$d = 2X\sqrt{1 - \left(\frac{\pi N X}{4}\right)^2} \tag{8}$$

Substituting the value for N given by equation (7) into equation (8)

$$d = 2X\sqrt{1 - (85.73963)X^2} \tag{9}$$

This expression can now be solved for values of d and X at which limit-cycle oscillation will occur. Values of d and X which satisfy this relationship are shown in figure 27, for two different values of the parameter N. As seen, a maximum d for each value of N can be obtained above which no limit-cycle oscillation will occur.

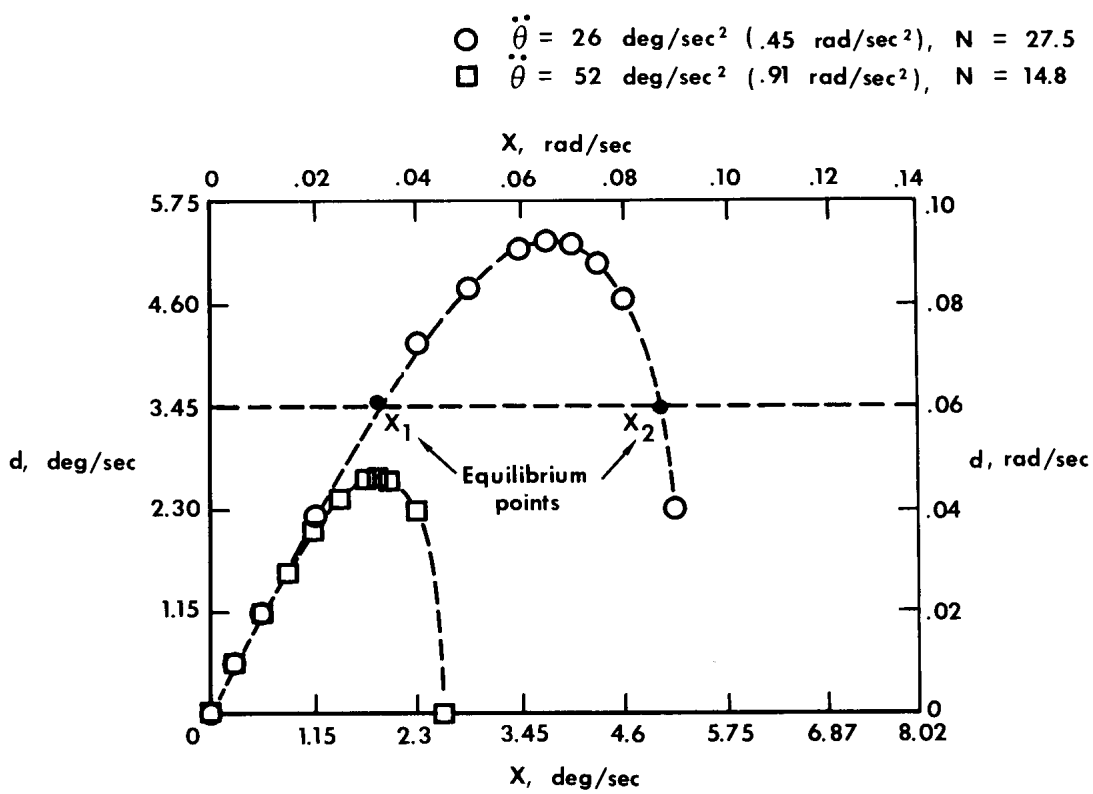

Figure 27.– Effect of rate dead band on limit-cycle amplitude.

Figure 27 also indicates the existence of two distinct limit-cycle amplitudes for each value of d. These two values of X correspond to stable and unstable equilibrium conditions and can be evaluated by the method presented in reference 15. By assuming a value of d = 3.45 deg/sec (0.06 rad/sec), two possible values of X are indicated in the figure: X_1 = 1.89 deg/sec (0.03 rad/sec), and X_2 = 5.04 deg/sec (0.09 rad/sec). The amplitude most likely to result can be determined by means of the Bode plot of G(s) and $\left|\frac{1}{N}\right|$ in figure 28. The $\frac{1}{N}$ amplitude function is drawn at the phase crossover point of G(s) (phase goes through -180° (3.14 rad)), since this is the only frequency at which limit cycles are possible for a variable-gain nonlinearity. The $\left|\frac{1}{N}\right|$ curve has been separated into descending and ascending gain portions for clarity, since the function is double valued.

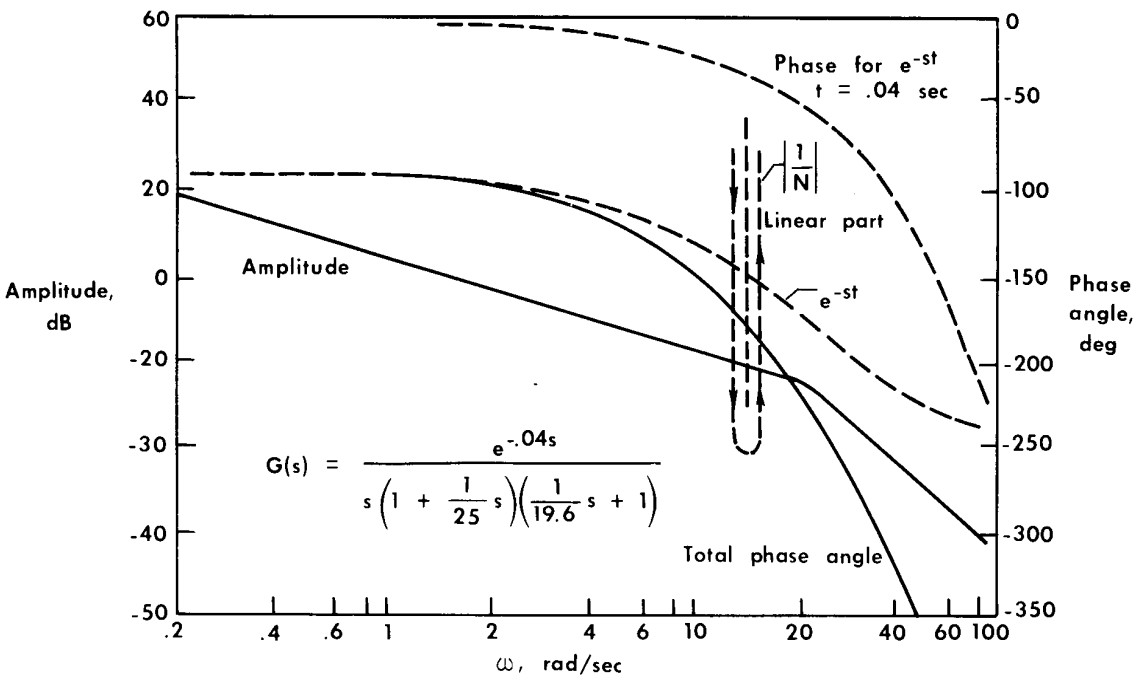

Figure 28.– Gain-phase plot of linear transfer function and nonlinear describing function.

As indicated in reference 15, for values of X less than X_1, the system is stable and small disturbances will not lead to an instability if the system is initially at rest. For an input signal into the system resulting in an $X = X_1$ input to the nonlinear element, sustained oscillations will occur at a frequency of ω = 13.5 rad/sec.

For a slightly larger input signal, the open-loop gain of the system will be driven greater than unity at the phase crossover point, resulting in an instability. The oscillation will then increase in amplitude until the equilibrium point X_2 is reached

and a sustained constant-amplitude oscillation is maintained. For inputs resulting in $X > X_2$, a stable system results and the oscillation decays back to the point X_2. Points X_1 and X_2, therefore, in figure 27 represent unstable and stable limit-cycle conditions, respectively. Since the probability that an unstable limit-cycle condition will occur for any extended time is extremely remote, only the oscillations occurring at the stable equilibrium point are usually considered.

REFERENCES

1. Hill, J. A.: A Piloted Flight Simulation Study To Define the Handling Qualities Requirements for a Lunar Landing Vehicle. Rep. No. NA 62H-660, North American Aviation, Inc., Sept. 13, 1962.

2. Garren, John F., Jr.; Kelly, James R.; and Reeder, John P.: A Visual Flight Investigation of Hovering and Low-Speed VTOL Control Requirements. NASA TN D-2788, 1965.

3. Rolls, L. Stewart; Drinkwater, Fred J., III; and Innis, Robert C.: Effects of Lateral Control Characteristics on Hovering a Jet Lift VTOL Aircraft. NASA TN D-2701, 1965.

4. Dathe, H. M.: Review of Hovering Control Requirements for VTOL Aircraft by a Flight Dynamics Analysis. AGARD Rep. 472, July 1963.

5. Mechtly, E. A.: The International System of Units - Physical Constants and Conversion Factors. NASA SP-7012, 1964.

6. Bellman, Donald R.; and Matranga, Gene J.: Design and Operational Characteristics of a Lunar-Landing Research Vehicle. NASA TN D-3023, 1965.

7. Jarvis, Calvin R.: Operational Experience With the Electronic Flight Control Systems of a Lunar-Landing Research Vehicle. NASA TN D-3689, 1966.

8. Cheatham, Donald C.; and Hackler, Clarke T.: Handling Qualities for Pilot Control of Apollo Lunar-Landing Spacecraft. J. Spacecraft Rockets, vol. 3, no. 5, May 1966, pp. 632-638.

9. Besco, Robert O.: Handling Qualities Criteria for Manned Spacecraft Attitude-Control Systems. J. Spacecraft Rockets, vol. 2, no. 4, July-Aug. 1965, pp. 628-630.

10. Faye, Alan E., Jr.: Attitude Control Requirements for Hovering Determined Through the Use of a Piloted Flight Simulator. NASA TN D-792, 1961.

11. Lineberry, Edgar C., Jr.; and Foudriat, Edwin C.: Application of Describing-Function Analysis to the Study of an On-Off Reaction-Control System. NASA TN D-654, 1961.

12. Ergin, E. I.; Norum, V. D.; and Windeknecht, T. G.: Techniques for Analysis of Nonlinear Attitude Control Systems for Space Vehicles. Tech. Doc. Rep. No. ASD-62-208, Vol. II, Aero. Sys. Div., U. S. Air Force, June 1962.

13. Jarvis, Calvin R.; and Lock, Wilton P., Jr.: Operational Experience With the X-15 Reaction Control and Reaction Augmentation Systems. NASA TN D-2864, 1965.

14. Stillwell, Wendell H.; and Drake, Hubert M.: Simulator Studies of Jet Reaction Controls for Use at High Altitude. NACA RM H58G18a, 1958.

15. Truxal, John G.: Automatic Feedback Control System Synthesis. McGraw-Hill Book Co., Inc., 1955.

TABLE I. – PILOT RATING SCALE

General classification	Numerical rating	Handling qualities	Ability to complete mission	Ability to land
Satisfactory	1	Easy to control precisely - little corrective control required.	Yes	Yes
	2	Good response but necessitates attention for precise control.	Yes	Yes
	3	Acceptable controllability but more than desired attention generally needed.	Yes	Yes
Unsatisfactory	4	Submarginal for normal use - requires excessive pilot attention.	Yes	Yes
	5	Controllability poor - demands constant pilot attention and continuous control inputs.	Probably	Yes
	6	Can be controlled, but pilot must exercise considerable care.	Doubtful	Yes
Unacceptable	7	Difficult to control and demands considerable pilot concentration.	No	Probably
	8	Controllable only with a high degree of pilot concentration and large control inputs.	No	Doubtful
	9	Extremely dangerous - can be controlled only with exceptional piloting skill.	No	No
	10	Uncontrollable.	No	No